

**NASA Contractor Report 189661**  
**ICASE Report No. 92-23**

P. 40

# ICASE

## STREAMWISE VORTICES IN HEATED BOUNDARY LAYERS

**Philip Hall**

Contract No. NAS1-18605  
June 1992

Institute for Computer Applications in Science and Engineering  
NASA Langley Research Center  
Hampton, Virginia 23665-5225

Operated by the Universities Space Research Association



National Aeronautics and  
Space Administration

**Langley Research Center**  
Hampton, Virginia 23665-5225

(NASA-CR-189661) STREAMWISE VORTICES IN  
HEATED BOUNDARY LAYERS Final Report (ICASE)  
40 p

N92-29692

Unclass  
G3/34 0109013



# STREAMWISE VORTICES IN HEATED BOUNDARY LAYERS

Philip Hall<sup>1</sup>

Department of Mathematics  
Manchester University  
Manchester M139PL ENGLAND

## ABSTRACT

The nonlinear instability of the boundary layer on a heated flat plate placed in an oncoming flow is investigated. Such flows are unstable to stationary vortex instabilities and inviscid traveling wave disturbances governed by the Taylor-Goldstein equation. For small temperature differences the Taylor-Goldstein equation reduces to Rayleigh's equation. When the temperature difference between the wall and free stream is small the preferred mode of instability is a streamwise vortex. It is shown in this case that the vortex, assumed to be of small wavelength, restructures the underlying mean flow to produce a profile which can be massively unstable to inviscid traveling waves. The mean state is shown to be destabilized or stabilized to inviscid waves depending on whether the Prandtl number is less or greater than unity.

---

<sup>1</sup>This research was supported by the National Aeronautics and Space Administration under NASA Contract No. NAS1-18605 while the author was in residence at the Institute for Computer Applications in Science and Engineering (ICASE), NASA Langley Research Center, Hampton, VA 23665.



## 1. Introduction

Our concern is with the nonlinear instability of forced convection boundary layers over horizontal heated flat plates and the subsequent secondary instabilities of these flows. In a previous paper, Hall and Morris (1992), hereafter referred to as HM, considered the linear aspects of longitudinal vortex instabilities. In general it was shown that this convective instability develops in a nonparallel manner and cannot be adequately described by a quasi-parallel stability theory of the type discussed by for example Wu and Cheng (1976), Moutsoglou, Chen and Cheng (1984), Chen and Cheng (1981). At higher values of the controlling stability parameter, the Grashof number, nonparallel effects can be taken care of in a self-consistent asymptotic manner provided that the vortex wavelength is not too large. In the present paper we will be concerned with extending the work of HM into the strongly nonlinear regime, in addition we will be concerned with the subsequent three-dimensional unsteady breakdown of the flow induced by large amplitude vortex structures.

In addition to longitudinal vortex structures both Tollmien-Schlichting and inviscid waves are possible causes of instability in a heated boundary layer. If buoyancy forces are not too large, then the inviscid modes are found to satisfy Rayleigh's equation, otherwise they satisfy the Taylor-Goldstein equation. We show that, when buoyancy forces are sufficiently large enough to alter the zeroth order inviscid instability problem, they also enter the equations for the basic state and cause the mean velocity and temperature fields to be coupled.

In order to make progress with an analytical solution of the strongly nonlinear instability problem associated with longitudinal vortex instabilities, we use the asymptotic structure given by Hall and Lakin (1988) in the context of small wavelength Görtler vortices. In this limit, which corresponds to the far downstream behavior of a fixed wavelength vortex, the vortices are confined to a finite part of the boundary layer and indeed where they exist the mean state adjusts to allow them to remain neutral. We show that in forced convection boundary layers the vortices occupy a region adjacent to the wall and that the thickness of this region increases linearly with Grashof number. The results we present are for similarity solutions of the nonlinear vortex-mean flow interaction problem but previous experience with the related Görtler problem, Hall (1988), Hall and Lakin (1988) suggests that the structure of the nonsimilar solutions is not significantly different.

A significant result which we find is that for Prandtl numbers less than unity favorable pressure gradient flows can have inflectional streamwise mean velocity profiles induced by vortices. This suggests that a major role of vortex instabilities might be to modify favorable pressure gradient flows to make them unstable to the relatively much more dangerous inviscid instabilities. We investigate the Rayleigh instability problem for such flows and show that vortices induce a class of unstable Rayleigh waves over a large range of wavenumbers.

The procedure adopted in the rest of this paper is as follows: in §2 we formulate the nondimensional equations governing vortex instabilities in heated boundary layers. In §3 these equations are solved for small vortex wavelengths and in §4 a similarity solution is obtained. Some large Grashof number properties of the similarity solution are discussed in §5 where we show the importance of the Prandtl number in determining the shape of the induced mean flow. In §6 we discuss the inviscid instability of the vortex states discussed in §3, 4, 5 and finally in §7 we draw some conclusions.

## 2. Formulation

Consider the viscous flow over a semi-infinite flat plate with a typical lengthscale  $L$  in the flow direction. Suppose that the fluid speed at infinity is  $U_0 u_e(x^*/L)$  where  $x^*$  measures distance along the wall. We define the parameters  $R$  and  $G$  by

$$R = U_0 L \nu^{-1}, \quad G = L^3 g (T_0 - T_\infty) \beta \nu^{-2} R^{-3/2}. \quad (2.1a, b)$$

Here  $\nu$  is the kinematic viscosity,  $g$  the acceleration due to gravity and  $\beta$  is the coefficient of expansion of the fluid. The temperatures  $T_0$  and  $T_\infty$  respectively denote a constant reference temperature and the fluid temperature in the freestream. We concern ourselves with the limit  $R \rightarrow \infty$  with  $G$  held fixed and determine the strongly nonlinear vortex flows which occur in this limit.

Suppose next that the wall temperature is given by

$$T = T_\infty + (T_\infty - T_0) \mathcal{T}(x^*/L) \quad (2.2)$$

and that we define dimensionless variables  $(x, y, z)$  by

$$(x, y, z) = (x^* L^{-1}, y^* L^{-1} R^{1/2}, z^* L^{-1} R^{1/2}), \quad (2.3)$$

where  $y^*, z^*$  denote distance in the normal and spanwise directions respectively. We define a dimensionless velocity field  $(u, v, w)$  associated with  $(x, y, z)$  by writing

$$(u^*, v^*, w^*) = U_0 (u, R^{-1/2} v, R^{-1/2} w). \quad (2.4)$$

The pressure  $p^*$  is then written in the form

$$p^* = \bar{\rho} U_0^2 \left\{ \bar{p}_0(x) + \bar{p}_1(x)/R^{1/2} + \frac{G}{R} \bar{p}(x, y) + \frac{p(x, y, z)}{R} + \dots \right\}, \quad (2.5)$$

where  $\bar{\rho}$  is a typical fluid density. The fluid density is given by

$$\rho^* = \bar{\rho} [1 + \bar{\beta} (T^* - T_\infty)] \quad (2.6)$$

and we shall make the Boussinesq approximation throughout this work so that changes in  $\rho$  can be ignored unless they are multiplied by gravity. The temperature field is then made dimensionless by writing

$$T^* = T_\infty + (T_0 - T_\infty)T. \quad (2.7)$$

In the Boussinesq approximation the continuity equation, momentum equations and energy equations are:

$$\begin{aligned} \nabla \cdot \underline{u} &= 0, \\ (\underline{u} \cdot \nabla) \underline{u} &= \begin{bmatrix} -\bar{p}'_0(x) - \bar{p}'_1(x)R^{-1/2} - \bar{p}_x \frac{G}{R} - \frac{p_x}{R} \\ (-\bar{p}_y G + GT) - p_y \\ -p_z \end{bmatrix} + \nabla^2 \underline{u}, \\ (\underline{u} \cdot \nabla) T &= \frac{1}{\sigma} \nabla^2 T, \end{aligned} \quad (2.8a, b, c)$$

where  $\sigma$  is the Prandtl number,  $\nabla \equiv (\partial_x, \partial_y, \partial_z)$  and  $\nabla^2 = (\partial_y^2 + \partial_z^2 + R^{-1} \partial_x^2)$ . The boundary conditions appropriate to (2.8) are

$$\begin{aligned} \underline{u} &= 0, \quad T = T(x), \quad y = 0, \\ u &\rightarrow u_e, \quad w \rightarrow 0, \quad T \rightarrow 0, \quad y \rightarrow \infty. \end{aligned} \quad (2.9a, b)$$

Note here that if the instability is caused by for example nonuniform wall heating the conditions at the wall should be modified as in HM. In the absence of any instabilities we write  $\underline{u} = (\bar{u}, \bar{v}, 0)$ ,  $T = \bar{T}$  and the basic state is determined in the limit  $R \rightarrow \infty$  by

$$\left. \begin{aligned} \bar{u}_x + \bar{v}_y &= 0, \\ \bar{u}\bar{u}_x + \bar{v}\bar{u}_y &= u_e u_{ex} + \bar{u}_{yy} - S\bar{p}_x \\ \bar{p}_y &= \bar{T}, \\ \bar{u}\bar{T}_x + \bar{v}\bar{T}_y &= \frac{\bar{T}_{yy}}{\sigma}, \\ \bar{u} = \bar{v} = 0, \quad \bar{T} &= T, y = 0, \\ \bar{u} &\rightarrow u_e, \quad \bar{T} \rightarrow 0, y \rightarrow \infty. \end{aligned} \right\} \quad (2.10a - f)$$

Here we have set  $\bar{p}_{0x} = -u_e u_{ex}$  and introduced the buoyancy parameter  $S = G/R$  which we take to be  $O(1)$ . The longitudinal vortex structure of HM first occurs for  $G = O(R^\circ)$  but our

ultimate concern is with the interaction of vortex structures and Taylor-Goldstein inviscid waves which exist for  $G/R \sim 0(R^0)$ . Hence it is convenient at this stage to allow for a ‘buoyancy’ coupling between the  $x, y$  momentum equations, even though most of the results given in this paper will be for the case  $S = 0$ . Note also that (2.10c) can be integrated and the result substituted into (2.10b) to give

$$\bar{u}\bar{u}_x + \bar{v}\bar{u}_y = u_e u_{ex} + \bar{u}_{yy} + S \int_{\infty}^y \bar{T}_x dy. \quad (2.11)$$

This coupling has a significant effect on similarity solutions for the basic state. In particular if we choose  $u_e = x^n$  then the wall temperature  $T$  must be proportional to  $x^{5n/2-1/2}$  for a similarity solution to exist.

In HM the linearized version of (2.8) was solved for the case  $n = 1$ ; it was shown that at  $O(1)$  values of  $G$  the longitudinal vortex instability induced by heating develops in a nonparallel manner. At higher values of  $G$  interest centres on the right-hand branch of the neutral curve where vortices of wavenumber  $a$  are neutral for  $G \sim a^4$ . In fact this high wavenumber regime is important because a disturbance of fixed physical wavelength will correspond to large values of the local Grashof and wavenumbers at sufficiently large values of  $x$ . Thus the regime is particularly relevant to experiments where the vortex instability is caused by very small background disturbances which must evolve over a significant distance before they develop in a nonlinear manner. It is with the latter nonlinear problem which we will concern ourselves in this paper.

### 3. The Strongly Nonlinear Evolution Equations for Small Wavelength Streamwise Vortices

The nonlinear structure which we develop in this section is based on the related analysis of Hall and Lakin (1988) for Görtler vortex flows. The major difference between the problems however is that in the convection problem small wavelength neutral vortices occur near to the boundary whilst in the Görtler problem the vortices move away from the wall to the position in the flow where Rayleigh’s criterion is most violated. This difference leads to significant differences in the corresponding nonlinear structures. In fact the heated boundary layer has some similarities with the strongly nonlinear Taylor vortex problem, Denier (1992). However, the fact that the Taylor instability occurs in a bounded region causes even the Taylor and convection problems to differ significantly at high values of the appropriate control parameters.

In the convection problem, small wavelength vortices feel the local strength of the destabilizing buoyancy force through  $\frac{\partial T}{\partial y}$ , the vertical gradient of the basic temperature field. In general, this gradient is a maximum at the wall so the instability is initiated there. In fact



it was shown in HM that in the neutral case the dominant balance is between spanwise diffusion and buoyancy effects in the  $y$  momentum equation and between spanwise diffusion and the convective operator in the energy equation. It is this balance which leads us to the appropriate generalization of Hall and Lakin (1988) to the present problem.

Suppose then that a vortex of wavelength  $a$  exists in a region of depth  $0(1)$  adjacent to  $y = 0$ . Since we have assumed that  $G/R$  is  $0(1)$  then we must consider the case when  $a = 0(R^{1/4})$ . Thus we write

$$G = \hat{G}a^4 + \dots \quad (3.1a, b)$$

$$\text{with } G/R = S + \dots$$

In order to recover the situation when buoyancy is not important we must then consider the second limit  $S \rightarrow 0$ . The neutral right hand branch modes for  $a \gg 1$  have temperature, pressure and velocity perturbations  $\hat{\theta}, \hat{p}, \hat{u}, \hat{v}, \hat{w}$  such that

$$\frac{\hat{v}}{\hat{\theta}} \sim 0(a^2), \quad \frac{\hat{v}}{\hat{p}} \sim 0(1), \quad \frac{\hat{v}}{\hat{u}} \sim 0(a^2), \quad \frac{\hat{v}}{\hat{w}} \sim 0(a). \quad (3.2)$$

The first of the above scalings follows from our earlier remarks concerning the balances  $G\hat{\theta} \sim \hat{v}_{zz}$ ,  $\hat{\theta}_{zz} \sim \hat{v}\bar{T}_y$  whilst the remaining balances follow from the choice of balances  $p_z \sim w_{zz}$ ,  $u_{zz} \sim v\bar{u}_y$ ,  $v_y \sim w_z$  in the  $z, x$  momentum equations and the continuity equation respectively. We then fix the overall size of the disturbance so that the mean flow and temperature field corrections driven by the disturbance are comparable with the unperturbed flow. Thus we require that  $\hat{u} \cdot \nabla \hat{u} \sim 0(1) \sim \hat{u} \cdot \nabla \hat{\theta}$ ; we therefore expand  $u, v, w, p$  and  $T$  appearing in (2.8) in the form

$$\begin{aligned} u &= \bar{u}_0 + a^{-2/3}\bar{u}_1(x, y) + \dots + a^{-1}[U_0(x, y)E + C.C.] + \dots \\ v &= \bar{v}_0 + a^{-2/3}\bar{v}_1(x, y) + \dots + a[V_0(x, y)E + C.C.] + \dots \\ w &= [W_0(x, y)E + C.C.] + \dots \\ p &= [a^2P_0(x, y)E + C.C.] + \dots \\ T &= \bar{T}_0(x, y) + a^{-2/3}\bar{T}_1(x, y) + \dots + a^{-1}[\theta_0E + C.C.] + \dots \end{aligned} \quad (3.3a, b, c, d, e)$$

In the above expressions the function  $2E = e^{iaz}$ ,  $C.C.$  denotes complex conjugate and  $\dots$  denotes terms smaller (in terms of  $a$ ) than those immediately before this symbol. Notice also that the mean (in terms of  $z$ ) part of the pressure must be expanded as

$$\bar{p} = \bar{q}_0(x, y) + a^{-2/3}\bar{q}_1(x, y) + \dots \quad (3.3f)$$

Furthermore, we have anticipated that the correction terms in (3.3) to the mean and fundamental are  $0(a^{-2/3})$  smaller than the dominant terms. This choice can be inferred from the

fact that the correction terms to the mean must be comparable to the depth of the transition layer in which the vortices decay to zero. Since the depth of this layer is governed by the scalings of the linear neutral problem it must be of depth  $0(a^{-2/3})$ , see Hall and Lakin (1988).

#### Equations for the vortex

If we substitute (3.3) into (2.8) and retain the leading order fundamental terms we obtain:

$$\begin{aligned}
V_{0y} + iW_0 &= 0, \\
U_0 + V_0 \bar{u}_{0y} &= 0, \\
\hat{G}\theta_0 - V_0 &= 0, \\
W_0 + iP_0 &= 0, \\
\frac{\theta_0}{\sigma} + V_0 \bar{T}_{0y} &= 0.
\end{aligned} \tag{3.4a, b, c, d, e}$$

These equations determine only  $U_0, V_0, W_0$ , and  $P_0$  in terms of  $\theta_0$ , and in fact the equations are only consistent if

$$\sigma \hat{G} \bar{T}_{0y} + 1 = 0.$$

We integrate this equation to give

$$\bar{T}_0 = \mathcal{T}(x) - \frac{y}{\hat{G}\sigma}, \tag{3.4f}$$

where we have satisfied the required boundary condition on  $\bar{T}_0$  at  $y = 0$ . The temperature profile (3.4f) is that temperature distribution which enables a vortex of wavenumber  $a \gg 1$  to remain neutral. Without any loss of generality we will now assume that the fundamental temperature disturbance  $\theta_0$  is real.

#### Equations for the mean:

If we substitute the expansions (3.3) into (2.8) and equate the leading order mean terms in the continuity,  $x, y$  momentum equations and the energy equations and use (3.3) we obtain

$$\begin{aligned}
\bar{u}_{0x} + \bar{v}_{0y} &= 0, \\
\bar{u}_0 \bar{u}_{0x} + \bar{v}_0 \bar{u}_{0y} &= -S \bar{q}_{0x} + u_e u_{ex} + \bar{u}_{0yy} + \frac{1}{2} \left\{ \bar{u}_{0y} V_0^2 \right\}_y, \\
\bar{q}_{0y} &= \bar{T}_0 \\
\bar{u}_0 \bar{T}_{0x} + \bar{v}_0 \bar{T}_{0y} &= \frac{1}{\sigma} \bar{T}_{0yy} + \frac{\sigma}{2} \left\{ \bar{T}_{0y} V_0^2 \right\}_y.
\end{aligned} \tag{3.5a, b, c, d}$$

The  $y$ -momentum equation above can be integrated directly to give

$$\bar{q}_0 = \int_0^y \bar{T}_0 dy + \bar{q}_0(x, 0). \quad (3.5e)$$

The function  $\bar{T}_0$  appearing in (3.5c) can then be replaced by  $1 - \frac{y}{\hat{G}\sigma}$  and then (3.5a,b,d) can be integrated to find  $V_0^2, \bar{u}_0, \bar{v}_0$ . It is instructive at this stage to seek a similarity solution of (3.5) in order to gain some insight into the nonlinear structure we have obtained.

We recall that for the Falkner-Skan profile with  $u_e \sim x^n$  buoyancy forces can only be retained within the similarity solution structure if  $T \sim x^{\frac{5n-1}{2}}$ . However (3.4c) implies that a similarity solution in the presence of vortices is possible only if  $T \sim x^{(1-n)/2}$ . Thus a similarity solution in the presence of both buoyancy effects and vortices is possible only if  $n = 1/3$ . In fact the case  $n = 1/3$  is of particular interest in vortex-wave interaction theory, since, as will be remarked upon later, the only possible similarity solution when small wavelength vortices interact with Rayleigh or Taylor-Goldstein waves has  $n = 1/3$ . In the next section we will discuss the  $n = 1/3$  case in detail, before doing so we will complete the description of the flowfield for the more general non self-similar case. However we stress that the results which we obtain for this particular choice of  $n$  are typical of the other similarity solutions.

The equations (3.5a,b,d) must in general be integrated numerically with  $\bar{q}_0$  given by (3.5c) and  $\bar{T}_0$  given by (3.4f). However, we can think of (3.5d) as a first order equation in  $y$  for  $V_0^2$  and we formally write the solution in the form

$$V_0^2 = V_0^2(x, 0) - 2\hat{G} \int_0^y \left[ \bar{u}_0 \mathcal{T}_x - \frac{\bar{v}_0}{\hat{G}\sigma} \right] dy. \quad (3.6)$$

The function  $V_0(x, 0)$  remains unknown at this stage and for small values of  $y$  the integrand behaves like  $\bar{u}_{0y}(x, y)y\mathcal{T}_x$  so that if we assume there is no reversed flow then this quantity is positive if  $\mathcal{T}_x > 0$ . Thus for similarity solutions with  $n < 1$ ,  $V_0^2$  is a positive decreasing function near the wall and we expect that, since we do not anticipate the presence of vortices everywhere, the vortex will vanish at some value of the similarity variable  $\eta$ . In fact for similarity solutions with values of  $n$  not satisfying this inequality the integrand becomes positive for large enough  $\eta$ , thus the only major change is that the maximum of  $V_0$  occurs away from the wall. We also expect that (3.6) will determine  $V_0^2$  in a finite range of values for  $y$  in the non self-similar case.

The solution (3.6) is therefore valid for  $0 < y < \bar{y}$  and more precisely near  $\bar{y}$ ,  $V_0 \sim |y - \bar{y}|$  and viscous effects come back into play. In fact a layer of depth  $a^{-2/3}$  is required at  $\bar{y}$  in order to allow  $V_0$  to adjust from algebraic decay for  $\bar{y} - y \gg a^{-2/3}$  to exponential decay for  $y - \bar{y} \gg a^{-2/3}$ . The required structure in this layer is virtually identical to that given by Hall and Lakin (1988) and so will not be repeated here. It suffices to say that  $V_0$  satisfies the second Painleve equation in this layer and that across the layer  $\bar{u}_0, \bar{u}_{0y}, \bar{v}_0, \bar{T}_0, \bar{T}_{0y}$  and  $\bar{q}_0$

are continuous. Thus above the transition layer we retain the expansions (3.3) but with all the  $z$  dependent terms set equal to zero so that the leading order problem for  $\bar{u}_0, \bar{v}_0$ , etc. in this upper layer is identical to that for the unperturbed flow. We can therefore write down the following 'composite' problem for the whole flow field.

$$\left. \begin{aligned} \bar{u}_{0x} + \bar{v}_{0y} &= 0, \\ \bar{u}_0 \bar{u}_{0x} + \bar{v}_0 \bar{u}_{0y} &= -S \bar{q}_{0x}(x, 0) - S \int_0^y \bar{T}_{0x} dy + u_\epsilon u_{\epsilon x} + \bar{u}_{0yy} \\ &\quad + \frac{1}{2} H(V_0^2) \{ \bar{u}_{0y} V_0^2 \}_y, \\ \bar{u}_0 \bar{T}_{0x} + \bar{v}_0 \bar{T}_{0y} &= \frac{1}{\sigma} \bar{T}_{0yy} + \frac{\sigma}{2} H(V_0^2) \{ \bar{T}_{0y} V_0^2 \}_y, \\ H(V_0^2) \left\{ \bar{T}_0 - \mathcal{T}(x) + \frac{y}{\hat{G}\sigma} \right\} &= 0, \end{aligned} \right\} \quad (3.7)$$

where  $H$  is the Heaviside function

$$H(s) = \begin{cases} 1, & s > 0 \\ 0, & s \leq 0. \end{cases}$$

The appropriate boundary conditions are

$$\left. \begin{aligned} V_0 &= V_0(x, 0), \bar{u}_0 = \bar{v}_0 = 0, \bar{T}_0 = \mathcal{T}, y = 0 \\ \bar{u}_0 &\rightarrow u_\epsilon, \bar{T}_0 \rightarrow 0, y \rightarrow \infty \\ \text{and } \bar{q}_{0x}(x, 0) &= -\int_0^\infty \bar{T}_{0x} dy. \end{aligned} \right\} \quad (3.8)$$

We note that at the point  $\bar{y}$  where  $V_0^2 = 0$  the functions  $\bar{u}_0, \bar{u}_{0y}, \bar{v}_0, \bar{T}_0, \bar{T}_{0y}$  are to be made continuous and, since  $(\bar{u}_0, \bar{T}_0) \rightarrow (u_\epsilon, 0)$  as  $y \rightarrow \infty$ , then  $V_0(x, 0), \bar{u}_{0y}(x, 0)$ , must adjust themselves in order that this limit is achieved. Note also that the position  $\bar{y}$  where  $V_0$  vanishes will also be a function of  $x$ . In fact for numerical reasons it is more convenient to treat  $\bar{q}_{0x}(x, 0)$  as a third unknown to be iterated upon until  $\bar{q}_0(x, 0) + \int_0^\infty \bar{T}_0 dy = 0$ . The numerical free boundary value problem specified by (3.7, 3.8) can be solved in principle by adapting the procedure described in Hall and Lakin (1988), however it was found in that paper that the form of the non-self-similar solution can be inferred from the self-similar ones by varying the parameter corresponding to  $\hat{G}$ .

It remains for us to discuss the nature of the flow described above in the neighborhood of the wall. We recall that the solution which we have obtained has  $\bar{u} = \bar{v} = 0, \bar{T}_0 = \mathcal{T}$  at

the wall but  $V_0(x, 0) \neq 0$ . Of course the total flow must satisfy the no-slip conditions at the wall so an inner boundary layer must be present as the wall is approached. We can see from (3.3a) that in the limit  $y \rightarrow 0$  the solution calculated above is such that

$$u \sim y\bar{u}_{0y}(x, 0) + \cdots + a^{-1}[U_0(x, 0)E + \cdots] \cdots$$

which suggests that a new structure will emerge when  $y$  falls to  $0(a^{-1})$ . Thus we define a new variable  $\zeta$  by

$$\zeta = ay$$

and seek a solution for  $\zeta = 0(1)$ . An examination of the higher harmonics in (3.3), which are smaller than the fundamental for  $y = 0(1)$ , shows that for  $\zeta = 0(1)$  all modes are comparable. This is because the cascade of energy from the fundamental down to the harmonics is enhanced to such an extent by the vertical diffusion of vorticity, now comparable with spanwise diffusion, that the energy in the different modes is of a similar size.

Thus in the neighborhood of the wall we must replace (3.3) by

$$\begin{aligned} u &= a^{-1}\hat{u}(x, \zeta, z) + 0(a^{-5/3}), \\ v &= a\hat{v}(x, \zeta, z) + 0(a^{1/3}), \\ w &= a\hat{w}(x, \zeta, z) + 0(a^{-2/3}), \\ p &= a^2\hat{p} + 0(a^{4/3}), \\ T &= \mathcal{T} + a^{-1}\hat{T}(x, \zeta, z) + 0(a^{-5/3}), \end{aligned} \tag{3.9a, b, c, d, e}$$

whilst  $\bar{p}$  now expands as

$$\bar{p} = \hat{q}(x, \zeta) + 0(a^{-2/3}).$$

The zeroth order approximation to (2.8) in the wall layer then becomes,

$$\begin{aligned} \hat{v}_\zeta + \hat{w}_z &= 0, \\ \hat{v}\hat{u}_\zeta + \hat{w}\hat{u}_z &= \hat{u}_{\zeta\zeta} + \hat{u}_{zz}, \\ \hat{v}\hat{v}_\zeta + \hat{w}\hat{v}_z &= \hat{G}\hat{T} - \hat{p}_\zeta + \hat{v}_{\zeta\zeta} + \hat{v}_{zz}, \\ \hat{v}\hat{w}_\zeta + \hat{w}\hat{w}_z &= -\hat{p}_z + \hat{w}_{\zeta\zeta} + \hat{w}_{zz}, \\ \hat{v}\hat{T}_\zeta + \hat{w}\hat{T}_z &= \frac{1}{\sigma} \{ \hat{T}_{\zeta\zeta} + \hat{T}_{zz} \}, \\ \hat{q}_\zeta &= 0 \end{aligned} \tag{3.10a, b, c, d, e, f}$$

which must be solved subject to

$$\hat{u} = \hat{v} = \hat{w} = 0,$$

$$\hat{u} \rightarrow \bar{u}_{0y}(x, 0)\zeta + [U_0(x, 0)E + C.C.], \quad \zeta \rightarrow \infty,$$

$$\hat{p} \rightarrow 0, \quad \zeta \rightarrow \infty,$$

$$\hat{v} \rightarrow [V_0(x, 0)E + C.C.], \quad \zeta \rightarrow \infty,$$

$$\hat{w} \rightarrow 0, \quad \zeta \rightarrow \infty,$$

$$\hat{q} \rightarrow \bar{q}_0(x, 0), \quad \zeta \rightarrow \infty.$$

and it is easy to show that a solution of the above system can be found by integrating from  $\zeta = \infty$  to  $\zeta = 0$  using an appropriate asymptotic form for  $\zeta \gg 1$ . Thus the wall boundary layer is passive even though it is fully nonlinear. Hence we can obtain the core solution for  $y = 0(1)$  without reference to the wall layer problem so we do not discuss further the latter problem. We shall now discuss self-similar solutions of the strongly nonlinear interaction problem (3.7) - (3.8).

#### 4. A Self-Similar Solution

We shall now concentrate on the special case

$$u_e = x^{1/3}, \quad \mathcal{T} = x^{1/3},$$

and introduce the similarity variable  $\eta$  defined by

$$\eta = \frac{y}{x^{1/3}}.$$

We then write

$$\bar{u}_0 = x^{1/3}f'(\eta), \quad \bar{v}_0 = \frac{1}{3x^{1/3}}\{\eta f' - 2f\}, \quad \bar{T}_0 = x^{1/3}g(\eta), \quad V_0 = \hat{V}(\eta), \quad q_0 = x^{2/3}q(\eta).$$

The free boundary problem (3.7) - (3.8) can then be written in the simplified ordinary

differential equation form:

$$\left. \begin{aligned} f''' + \frac{1}{3}\{2f''f - f'^2 + 1\} &= \frac{2}{3}Sq(\eta) - \frac{S\eta}{3}q' - \frac{H(\hat{V}^2)}{2}\{f''\hat{V}^2\}', \\ \frac{1}{\sigma}g'' - \frac{1}{3}\{f'g - 2fg'\} &= -\frac{\sigma}{2}H(\hat{V}^2)\{g'\hat{V}^2\}', \\ H(\hat{V}^2)\{g - 1 + \frac{\eta}{\hat{G}\sigma}\} &= 0, \\ q' &= g \\ f = f' &= 0, \eta = 0, f' = 1, q = g = 0, \eta = \infty. \end{aligned} \right\} \quad (4.1a, b, c, d, e)$$

In addition we require that  $f, f', q, g$  and  $g'$  are continuous at  $\eta = \bar{\eta}$  where  $\hat{V} = 0$ . The problem can be solved numerically by making guesses for  $\hat{V}(0), q(0), f''(0)$  and integrating (4.1a,b,d) to find  $\hat{V}, f$ , and  $q$  with  $g = 1 - \frac{\eta}{\hat{G}\sigma}$ . At the point where  $\hat{V} = 0$  we then set the terms proportional to  $\hat{V}^2$  in (4.1a,b) equal to zero and integrate these equations together with (4.1d) to determine  $f, g$  and  $q$  for  $\eta > \bar{\eta}$ . This integration is carried out using the computed values of  $f, f', f'', g, g'$  and  $q$  found as  $\eta \rightarrow \bar{\eta}$ . For arbitrary choices of  $\hat{V}(0), f''(0), q(0)$  the conditions  $f'(\infty) = 1, g(\infty) = 0, q(\infty) = 0$  will not be satisfied but we can perform a Newton iteration procedure on the wall values of  $\hat{V}, f'', g'$  until the conditions at infinity are satisfied.

Numerical solutions of (4.1) were in the first instance obtained for a range of values of  $\hat{G}$  for  $S = 0, \sigma = .2, 1, 5$ . In Figure 1 we show the computed values of  $\bar{\eta}, \hat{V}^2(0)$  and  $f''(0)$ . We see that solutions can be obtained for  $\hat{G}$  greater than some finite value, in fact this critical value corresponds to the right hand branch of the neutral curve. At the larger values of  $\hat{G}$  used in the calculations the results suggest that  $\bar{\eta} \sim \hat{G}, \hat{V}^2(0) \sim \hat{G}^2, f''(0) \sim \hat{G}^{-1}$ . We shall comment further on this asymptotic limit in the next section.

In Figures 2, 3, 4 we show the functions  $f', f'', g$  and  $\hat{V}^2$  in terms of  $\eta$  for different values of  $\hat{G}$  with  $\sigma$  respectively equal to 1, 5, .2. It can be seen in each case that the boundary layer thickens as the Grashof number increases. In Figures 2b, 4b we note the discontinuity in  $f'''$  which occurs at the transition layer position  $\eta = \bar{\eta}$ . The discontinuity also occurs for the case  $\sigma = 5$  shown in Figure 3b but at the values of  $\hat{G}$  used in the calculations the discontinuity is not apparent. In each of the calculations the function  $\hat{V}^2$  decreases monotonically from its value at the wall to zero at  $\eta = \bar{\eta}$ . The temperature profiles shown in Figures 2c, 3c, 4c illustrate the large  $\hat{G}$  structure mentioned above. Thus as  $\hat{G}$  increases the interval over which  $g$  is linear in  $\eta$  itself increases linearly with  $\hat{G}$ . On the other hand as  $\hat{G}$  is decreased towards its linear critical value the temperature profile approaches it's unperturbed form. It is also clear from the calculated velocity and temperature fields that an important consequence of

the mean flow being driven by the vortices is that the boundary layer thickness is increased from its unperturbed value. More precisely we note that in the presence of vortices the boundary layer thickness is increased by a factor  $\hat{G}$  from its unperturbed value.

A significant difference between the calculations for the different values of  $\sigma$  can be seen in Figures 2b, 3b, 4b. We refer to the fact that at the smallest value of  $\sigma$ , namely  $\sigma = .2$ , the function  $f''$  has a minimum in the region where the vortices exist and a discontinuity in the sign of its derivative across the transition layer. This result is significant because it means that the mean velocity profiles associated with  $f'$  have inflection points at the minima of  $f''$  and sign changes in the second derivative of the mean downstream velocity component at the transition layers. We stress that no such points were found for the cases  $\sigma = 1, 5$ , this suggests that inflection points can only be created by the vortices below some critical value of the Prandtl number. This means that in low Prandtl numbers flows, wall heating not sufficiently large to induce Taylor-Goldstein modes because  $S = 0$ , might still lead to highly unstable inviscid Rayleigh waves. The secondary instability of the flows induced by the vortices will be discussed in the final section of this paper.

In Figure 5 we show  $f'''$  as a function of  $\eta$  for the case  $\sigma = .2$ . We note that the size of the jump in  $f'''$  across the transition layer increases with  $\hat{G}$ . In addition when  $\hat{G}$  increases we see that the region between the wall and the inflection point increases but that  $f'''$  remains relatively small until the transition layer is reached. In order to understand this behavior it is instructive to consider the limit  $\hat{G} \rightarrow \infty$  in (4.1) and see how the underlying flow structure evolves. This limit will be discussed in the next section, before doing so we report on some calculations we have carried out for the case when buoyancy effects are present. In Figures 6a,b,c we show the quantities  $\bar{\eta}_1$ ,  $f''(0)$  and  $\hat{V}^2(0)$  for the case  $\sigma = 1$ , and  $S = 0, 1, 2$ . The velocity and temperature profiles associated with the  $S = 2$  calculations are shown in Figures 6d,e,f,g, we note here that the most significant difference between the  $S = 0$  and  $S = 2$  results is that buoyancy effects cause  $f'$  to overshoot its free-stream value for a range of values of  $\eta$ .

## 5. The Limiting $\hat{G} \rightarrow \infty$ Flow Structure

We stress here that, although our asymptotic analysis is carried out on the similarity problem discussed in Section 4, the approach can be applied in a similar way to the nonsimilar problem in the limit  $x \rightarrow \infty$  with  $\hat{G}$  fixed, see §7 for a brief discussion of this situation.

In order to develop a large  $\hat{G}$  solution of (4.1) it is first convenient to write (4.1a,c) in



the form

$$\begin{aligned} \left(\frac{\hat{V}^2}{2}\right)' &= \frac{-1}{3\sigma} \{(\hat{G}\sigma - \eta)f' + 2f\}, \\ f''' &= \frac{\frac{\sigma}{3}\{(f'^2 - 1 - 2ff'')\} + \frac{f''}{3}\{(\hat{G}\sigma - \eta)f' + 2f\}}{\sigma \left[1 + \frac{\hat{V}^2}{2}\right]}, \end{aligned} \quad (5.1a, b)$$

which are valid if  $\hat{V}^2 > 0$ .

The numerical results discussed in the previous section suggested that for  $\hat{G} \gg 1$  the vortices are distributed over a region of depth  $0(\hat{G})$ . Hence we seek a solution of (5.1) with  $\eta = 0(\hat{G})$ . Actually, since  $\hat{G}$  is always multiplied by  $\sigma$  when it appears, it is more convenient to treat  $\sigma\hat{G}$  as a large parameter and define

$$\psi = \frac{\eta}{\hat{G}\sigma}. \quad (5.2a)$$

It then follows that the right and left hand sides of (5.1b) will balance if  $f \sim \hat{G}\sigma$ ,  $\hat{V} \sim \hat{G}\sigma$ , we therefore write

$$\begin{aligned} f &= \hat{G}\sigma\Psi(\psi) + \dots, \\ \hat{V} &= \hat{G}\sigma\tilde{V}(\psi) + \dots, \end{aligned} \quad (5.2b, c)$$

and the zeroth order problem obtained from substituting the above expansions into (5.1) is

$$\begin{aligned} \Psi''' &= \left(\frac{2}{3\sigma}\right) \left\{ \sigma(\Psi'^2 - 1 - 2\Psi\Psi'') + \Psi''([1 - \psi]\Psi' + 2\Psi) \right\} \tilde{V}^{-2}, \\ \left(\frac{\tilde{V}^2}{2}\right)' &= -\frac{1}{3\sigma} \{[1 - \psi]\Psi' + 2\Psi\}. \end{aligned} \quad (5.3a, b)$$

If we assume that there is no sublayer structure near  $\psi = 0$  then (5.3) must be solved subject to

$$\Psi = \Psi' = 0, \quad \tilde{V}^2 = \tilde{V}^2(0), \quad \psi = 0 \quad (5.4)$$

and  $\tilde{V}(0)$  is a constant to be determined. It can be shown that for  $\eta > \hat{G}\sigma$ , where no vortices exist, a large  $(\hat{G}\sigma)$  solution of (4.1) can only be developed if  $f' \rightarrow 1$ ,  $g \rightarrow 0$ ,  $\eta \rightarrow (\hat{G}\sigma)_+$  so in addition to (5.4) we require

$$\Psi' = 1, \quad \tilde{V} = 0, \quad \psi = 1. \quad (5.5)$$

The nonlinear differential system specified by (5.3), (5.4), (5.5) can in general only be solved numerically and the solution will fix  $\tilde{V}(0)$  and  $\Psi''(0)$ . However the expansions (5.2b,c) are not uniformly valid as  $\psi \rightarrow 1_-$  because in that limit  $\tilde{V} \sim (1 - \psi)$  so the constant term in

the denominator of (5.1b) will be comparable with  $\hat{V}^2$  when  $1 - \psi \sim 0(G\sigma)^{-2}$ . In order to find the appropriate expansions in that layer we observe that in the neighborhood of  $\psi = 1$  we can write

$$\begin{aligned}\Psi &= \psi + \bar{\psi} + \tilde{\psi} \\ \frac{\tilde{V}^2}{2} &= -\frac{2}{3\sigma}[1 + \bar{\Psi}][\psi - 1] + \dots\end{aligned}\tag{5.6a, b}$$

where  $\bar{\psi}$  is a constant determined by the solution in  $0 < \psi < 1$  and  $\tilde{\psi}$  is given by

$$\tilde{\psi} = c(1 - \psi)^{1+\sigma}\tag{5.7}$$

where  $c$  is a constant. It follows that in the neighborhood of  $\psi = 1$  the expansion (5.2b) must be modified to give

$$f = \hat{G}\sigma \left[ 1 + \bar{\psi} - \frac{\phi}{(\hat{G}\sigma)^2} + \frac{\tilde{\psi}(\phi)}{(\hat{G}\sigma)^{2+2\sigma}} + \dots \right]\tag{5.8}$$

where  $\phi = (G\sigma)^2(1 - \psi)$ . The function  $\tilde{\psi}$  is then found to be given by

$$\tilde{\psi} = c \left[ \phi + \frac{3}{2\sigma(1 + \bar{\psi})} \right]^{1+\sigma}.\tag{5.9}$$

The expansion (5.8) is valid until  $\phi = 0$  where the vortex vanishes. The solution found above is then matched onto the solution of

$$f''' + \frac{1}{3}\{2ff'' - f'^2 + 1\} = 0$$

satisfying  $f'(\infty) = 1$ . However, this outer layer is passive and so we do not pursue the solution further here.

It follows from the large  $\hat{G}\sigma$  solution found above that if  $\sigma < 1$  in this limit  $\bar{u}'' \sim f'''$  is a maximum in the layer near  $\eta = \hat{G}\sigma$ . In fact from above it can be shown that for  $\phi = 0(1)$

$$f''' = -c(1 + \sigma)\sigma(\sigma - 1) \left( \phi + \frac{3}{2\sigma(1 + \bar{\psi})} \right)^{\sigma-2} (\hat{G}\sigma)^{2(1-\sigma)}.$$

Thus  $f'''$  becomes large if  $\sigma < 1$ , this is consistent with our numerical work. Numerical solutions of (5.3) suggest that the constant  $c$  is always positive so that  $f'''$  is positive or negative near  $\eta = \hat{G}\sigma$  depending on whether or not  $\sigma$  is less or greater than 1. Moreover, in the case  $\sigma < 1$ ,  $f'''$  attains its largest value near  $\eta = \hat{G}\sigma$  and this value  $\sim (\hat{G}\sigma)^{2(1-\sigma)}$ . Since we can show that the solution for  $\eta > \hat{G}_0$  must have  $f''' < 0$  we see that the results shown in Figure 4 which showed a jump in the sign of  $f'''$  at  $\bar{\eta}$  are confirmed and indeed a similar

result would be found for any value of  $\sigma < 1$ . Furthermore since a small  $\eta$  solution of (4.1) shows that  $f'''$  is positive near  $\eta = 0$ , the continuity of  $f'''$  in  $(0, \bar{\eta})$  implies the existence of an inflection point in the velocity profile for any Prandtl number less than unity.

Some numerical solutions of (5.3) are shown in Figures 7, 8, 9. Figure 7 shows  $\Psi''(0)$  and  $\tilde{V}(0)$  as a function of  $\sigma$ . The computed velocity field in the large  $\hat{G}\sigma$  limit similarly agrees well with the full solutions. Of particular interest is the dependence of the function  $\Psi'''$  on  $\psi$  and  $\sigma$ . In Figures 8a,b we show plots of  $\Psi'$  and  $\Psi'''$  as functions of  $\psi$  and  $\sigma$ . The results shown confirm that inflectional velocity profiles exist only for  $\sigma < 1$ . At finite values of  $\hat{G}\sigma$  our calculations suggest again that inflectional profiles exist only for  $\sigma < 1$  though an exhaustive check of this possibility in the  $\sigma - \hat{G}$  plane was not carried out. In the case  $\sigma \neq 1$  the results of Figure 7 suggest that for any  $\sigma > 1$ ,  $\Psi'''$  is always negative whilst for  $\sigma < 1$   $\Psi'''$  is positive in an interval  $(\psi^*, 1)$  for some  $\psi^* < 1$ . In order to demonstrate the behavior of  $\Psi'''$  near  $\sigma = 1$  we have in Figure 9 plotted results for the cases  $\sigma = .98, .99, 1, 1.01, 1.02$ . We see that  $\Psi'''$  tends to a negative constant as  $\Psi \rightarrow 1$  for  $\sigma = 1$ , whilst for  $\sigma$  slightly less than 1  $\Psi'''$  becomes large and positive in a small interval near  $\psi = 1$ . For  $\sigma$  slightly greater than 1 the function  $\Psi'''$  is always negative but increases significantly in magnitude near  $\psi = 1$ . We note that the finite value of  $\Psi'''$  for  $\sigma = 1$  occurs because the next correction term in (5.6a) when  $\sigma = 1$  is proportional to  $\psi^3$ . The implications of the above results for secondary instability theory will be discussed in §6.

## 6. Rayleigh or Taylor-Goldstein Inviscid Breakdown Induced by Streamwise Vortices

Now let us consider the inviscid instability of the finite amplitude vortex structures described in the previous section. The approach we take is based on the work of Hall and Horseman (1991) on the instability of Görtler vortices. The most important property of an inviscid instability in a boundary layer flow is that it operates on the same streamwise lengthscale as the boundary layer thickness. In terms of (2.8) this means that for the inviscid wave disturbance  $\frac{\partial}{\partial x} \sim R^{1/2}$ . In addition inviscid waves are time-dependent so that terms  $\underline{u}_t, T_t$  must be added to (2.8b,c). Thus we now write

$$\begin{pmatrix} u \\ v \\ w \\ p \\ T \end{pmatrix} = \begin{pmatrix} \bar{u}(x, y, z) \\ \bar{v}(x, y, z) \\ \bar{w}(x, y, z) \\ \bar{p}(x, y, z) \\ \bar{T}(x, y, z) \end{pmatrix} + \Delta e^{iR^{1/2}[\int^x \alpha(x) dx - \Omega t]} \begin{pmatrix} U(x, y, z) \\ R^{1/2}V(x, y, z) \\ R^{1/2}W(x, y, z) \\ RP(x, y, z) \\ \theta(x, y, z) \end{pmatrix} + \dots \quad (6.1)$$

Here the first term corresponds to the combined mean flow-vortex state driven by buoyancy effects whilst the second term represents an inviscid travelling wave disturbance of arbitrarily

small amplitude  $\Delta$ . We again denote the buoyancy parameter  $S = G/R$  and then substitute (6.1) into (2.8) and equate terms of order  $\Delta$ . In the limit  $R \rightarrow \infty$  the zeroth order approximation to this system is

$$\begin{aligned}
i\alpha V + V_y + W_z &= 0, \\
i\alpha(\bar{u} - c)U + V\bar{u}_y + W\bar{u}_z &= -i\alpha P, \\
i\alpha(\bar{u} - c)V &= -P_y + S\theta, \\
i\alpha(\bar{u} - c)W &= -P_z, \\
i\alpha(\bar{u} - c)\theta + V\bar{T}_y + W\bar{T}_z &= 0.
\end{aligned} \tag{6.2a, b, c, d, e}$$

Here we have replaced  $\frac{\Omega}{\alpha}$  by the wavespeed  $c$  and the appropriate boundary conditions are  $V = 0$ ,  $y = 0, \infty$ . With the function  $\bar{u}$  specified by the steady nonlinear vortex problem discussed earlier the system (6.2) and the boundary conditions constitute an eigenvalue problem

$$\alpha = \alpha(c, S).$$

Note that if the basic state is dependent only on  $x, y$  then (6.2) can be reduced to

$$(\bar{u} - c)(V_{yy} - \alpha^2 V) - \bar{u}_{yy}V = -\frac{S\bar{T}'}{\bar{u} - c}\bar{V}, \tag{6.3}$$

which is the so-called Taylor-Goldstein equation. If buoyancy forces are negligible,  $S = 0$ , (6.3) reduces to Rayleigh's equation. However when  $\bar{u}$  is a function of  $z$  no simple generalization of (6.3) is available, but we can eliminate  $U, V, W$  and  $\theta$  from (6.2) to give

$$\left(\frac{P_y}{[\bar{u} - c]^2}\right)_y + \left(\frac{P_z}{[\bar{u} - c]^2}\right)_z - \frac{\alpha^2 P}{[\bar{u} - c]^2} = S \left[ \frac{P_y \bar{T}_y + P_z \bar{T}_z}{[\bar{u} - c]^2 [S\bar{T}_y - \alpha^2(\bar{u} - c)^2]} \right]. \tag{6.4}$$

If  $S = 0$  the above equation reduces to the equation obtained by Hall and Horseman (1991) in their discussion of inviscid instabilities induced by Görtler vortices. The solution of (6.4) is of course a nontrivial task bearing in mind the fact that  $\bar{u}$  must in general be determined numerically. Here we shall concentrate on the case when  $S = 0$  so that we are in effect limiting our analysis to the determination of whether vortex instabilities induced by wall heating can trigger a rapidly growing Rayleigh instability. Thus we shall now confine our attention to the solution of the eigenvalue problem

$$\left(\frac{P_y}{[\bar{u} - c]^2}\right)_y + \left(\frac{P_z}{[\bar{u} - c]^2}\right)_z - \frac{\alpha^2 P}{[\bar{u} - c]^2} = 0 \tag{6.5}$$

$$P_y = 0, \quad y = 0, \quad P \rightarrow 0, \quad y \rightarrow \infty.$$

with  $\bar{u}(x, y, z)$  determined by the nonlinear vortex equations in the presence of wall heating but with  $S = 0$ . In particular we will investigate the case when  $\bar{u}$  corresponds to the small wavelength solution discussed in §3.4. We recall that in that limit vortices are confined to a region of depth  $O(1)$  adjacent to the wall with boundary layers of thickness  $a^{-1}$ ,  $a^{-2/3}$  at the wall and at the edge of the region of vortex activity respectively. Above the  $a^{-2/3}$  transition layer the flow is determined by the unperturbed boundary layer equations and the mean parts of  $\bar{u}$ ,  $\bar{u}_y$  with respect to  $z$  are continuous across the layer. It follows that a solution of (6.5) can be sought with no  $z$  dependence where vortices are absent. In the lower part of the boundary layer, where  $\bar{u}$  expands as in (3.3a), we find that  $P$  takes the form

$$P = P_0 + a^{-1}P_1 + a^{-2}P_2 + a^{-3}P_3 \cos az + a^{-3}P_4 + \dots \quad (6.6)$$

where  $P_0, P_1$  etc. depend only on  $x, y$ . If we expand  $\alpha, c$  in the form

$$(\alpha, c) = (\alpha_0, c_0) + a^{-1}(\alpha_1, c_1) + \dots \quad (6.7)$$

then we find that  $P_0, P_3$  satisfy

$$\left( \frac{P_{0y}}{[\bar{u}_0 - c_0]^2} \right)_y - \frac{\alpha^2 P_0}{[\bar{u}_0 - c_0]^2} = 0, \quad (6.8)$$

and

$$P_3 = -2(\bar{u}_0 - c_0)^2 \left( U_0 P_{0y} [\bar{u}_0 - c_0]^{-3} \right)_y. \quad (6.9)$$

Equation (6.8) is simply the Rayleigh equation for a unidirectional flow  $\bar{u}_0$  so that the vortex does not have a direct effect on the zeroth order Rayleigh problem. However it does have a significant indirect effect because  $\bar{u}_0$  is determined by the vortices. In the region above the  $a^{-2/3}$  transition layer (6.8) again gives the correct zeroth order approximation to the inviscid stability problem. Across the layer  $\bar{u}_0$ ,  $\bar{u}_{0y}$  are continuous whilst  $\bar{u}_{0yy}$  is discontinuous. In fact this discontinuity in  $\bar{u}_{0yy}$  is smoothed out within the transition layer by viscous effects. An examination of (6.5) in the transition layer shows that as long as  $c_0 \neq \bar{u}_0$  in this layer then  $P_0, P_{0y}$  are continuous across the layer. Similarly the  $a^{-1}$  wall layer is passive so that if we are not concerned with neutral waves propagating downstream with the mean downstream fluid speed in the transition layer then it is sufficient for us to solve (6.8) with  $\bar{u}_0$  determined by the vortices in  $0 < y < \bar{y}$  and by the boundary layer equations for  $y > \bar{y}$ . For definiteness we consider the case when  $\bar{u}_0$  has the similarity form discussed in §4. Thus we write  $\bar{u}_0 = x^{1/3} f'(\eta)$  with  $f$  determined by (4.1), it is convenient to rescale  $\alpha_0, c_0$  by writing

$$\alpha_0 = \hat{\alpha}_0 x^{-1/3}, \quad c_0 = \hat{c}_0 x^{1/3}$$

so that the eigenvalue problem  $\hat{\alpha}_0 = \alpha_0(\hat{c}_0, \hat{G})$  becomes

$$\left( \frac{P_{0\eta}}{[f' - \hat{c}_0]^2} \right)_\eta - \frac{\hat{\alpha}_0^2 P_0}{[f' - \hat{c}_0]^2} = 0$$

$$P_{0\eta} = 0, \quad \eta = 0, \quad P_0 \rightarrow 0, \quad \eta \rightarrow \infty. \quad (6.10)$$

In fact the similarity solution we have considered is particularly important in vortex-wave interaction theory. In the latter theory, see Hall and Smith (1991), a small amplitude Rayleigh or Tollmien-Schlichting wave system interacts with itself to drive a strong vortex field which itself acts back on the wavefield. In the present context a Rayleigh-vortex interaction occurs if  $\Delta$  in (6.1) is chosen appropriately. In this case the wave system drives the vortex in the critical layer and the fact that the wave system must remain neutral as it moves downstream means that similarity solutions of the inviscid equation describing the wave are possible only if  $n = \frac{1}{3}$ .

In the absence of wall heating the basic state has  $f'$  determined by the Falkner-Skan problems for a pressure gradient proportional to  $x^{-1/3}$ , and since the velocity profile is non-inflectional no unstable inviscid eigenvalues exist. We saw in the previous section that inflectional streamwise velocity profiles are generated by wall heating whenever the Prandtl number  $\sigma$  is less than unity.

In Figures 10, 11, 12, 13 we show results we have obtained by solving (6.10) for the case  $\sigma = .2$  and a range of values of  $\hat{G}$ . In our calculations we have kept  $\hat{\alpha}_0$  real and computed the corresponding complex value of  $\hat{c}_0$ . We see in Figure 10 that at each value of  $\hat{G}$  there is a band of unstable modes present to the right of a finite value of  $\hat{\alpha}_0$ . Each mode becomes neutral and disappears when the wavespeed is equal to the fluid speed at the inflection point of the velocity profile. Note here that all our calculations were for cases where such an inflection point exists, at sufficiently small values of  $\hat{G}$  the basic mean profile approaches its unperturbed values and no inflection points exist. The unstable mode persists for all  $\hat{\alpha}_0$  greater than the neutral value but has  $(\hat{\alpha}_0 \hat{c}_0)_i$  tending to zero as  $\hat{\alpha}_0 \rightarrow \infty$ , in this limit  $c_0$  approaches the fluid speed at the discontinuity in  $f'''$  at the transition layer. An analysis of that limit shows that the present analysis breaks down when  $\hat{\alpha}_0 = 0(\log a)$ . In this wavenumber regime the Rayleigh wave has a two layer structure (of depth  $a^{-2/3}, (\log a)^{-1}$ ) at the transition layer and is effectively zero elsewhere. We do not give details of the behavior for  $\hat{\alpha}_0 \sim |\log a|$  because the mode is neutral there and the most unstable growth rates occur for  $\hat{\alpha}_0 = 0(1)$ . We see that the wavenumber of the most unstable mode increases as the Grashof number increases, this is of course due to the thickening of the boundary layer. Some eigenfunctions associated with the modes are shown in Figures 12, 13. We see the concentration near  $\bar{\eta}$  of the eigenfunction of the second mode as its growth rate approaches zero at large  $\hat{\alpha}_0$ .

## 7. Conclusion

We have shown that wall heating produces large amplitude streamwise vortex structures which completely alter the boundary layer in which they develop. We have concentrated our attention on self-similar flows which enabled us to solve the mean flow-vortex interaction problem by reducing it to a set of nonlinear differential equations. A significant result which we found was that the mean-state modified at zeroth order can have inflection points whereas the unperturbed state does not. For the special case when the driving pressure gradient is proportional to  $x^{-1/3}$  we found that inflectional profiles are only generated when the Prandtl number is less than unity.

The importance of the inflectional profiles is that they are highly unstable to Rayleigh waves growing on a streamwise lengthscale  $O(R^{-1/2})$  shorter than that over which the near state develops. This means that a boundary layer inviscidly stable in the absence of wall heating can be made massively inviscidly unstable by streamwise vortex restructuring of the boundary layer. It is of course relevant to question whether the significantly different mean flow character corresponding to the cases  $\sigma < 1$ ,  $\sigma > 1$  is a function of the particular similarity flow considered. In order answer this question we note that the more general form of the similarity solution given by (4.1) with  $S = 0$  is

$$\begin{aligned}
 \eta &= yx^{\frac{n-1}{2}}, \\
 \bar{u}_0 &= x^n f'(\eta), \bar{v}_0 = -\frac{x^{n-1}}{2} \left[ \frac{n-1}{2} \eta f' + \frac{n+1}{2} f \right], \\
 V_0 &= \hat{V}(\eta), \bar{T}_0 = x^{\frac{1-n}{2}} g(\eta), \\
 f''' + \left\{ \frac{n+1}{2} f f'' - n f'^2 + n \right\} &= -\frac{1}{2} \{ f'' \hat{V}^2 \}' H(\hat{V}^2), \\
 \frac{1}{\sigma} g'' + \frac{n+1}{2} f g' + \frac{n-1}{2} f' g &= -\frac{\sigma}{2} \{ g' \hat{V}^2 \}' H(\hat{V}^2), \\
 H(\hat{V}^2) \left( g - 1 + \frac{\eta}{\hat{G}\sigma} \right) &= 0 \\
 f = f' = 0, \eta = 0, f' = 1, g = 0, \eta = \infty, \\
 f, f', g, g' &\text{continuous at } \eta = \bar{\eta}, \text{ where } \hat{V}(\bar{\eta}) = 0.
 \end{aligned} \tag{7.1}$$

In order to see whether inflectional profiles exist at large  $\hat{G}\sigma$  we can repeat the analysis of §5 by seeking a solution for  $\hat{\sigma}$ . The expansion procedure follows exactly that as of §5 and the key result is that the correction term  $\tilde{\psi}$  in (5.6a) is independent of  $n$  and again proportional

to  $(-\psi + 1)^{\sigma+1}$ . This means that  $f'''$  becomes large as  $\psi \rightarrow 1_-$  and changes sign when  $\sigma$  passes through 1. This result can be used to infer that  $f'''$  is positive as  $\psi \rightarrow 1_-$  for  $\sigma < 1$  and coupled with the fact that  $f'''$  must be negative for  $\eta > \bar{\eta}$  and for  $\eta \ll 1$  we find that for any  $n$  the large  $\hat{G}\sigma$  limit leads to inflectional profiles for  $\sigma < 1$ . This argument suggests that the results obtained for the special case  $n = 1/3$  are typical and that inflectional profiles are produced whenever  $\sigma < 1$  at sufficiently large values of  $\hat{G}_0$ . In fact the large Grashof number analysis of §5 can be reformulated as a large  $x$  asymptotic solution of the full interactive problem. This can be done for  $u_e \sim x^n, \mathcal{T} \sim x^m$  for any positive  $m$  and it is found that inflectional profiles are again only created for Prandtl numbers less than unity. This suggests that all heated boundary layer flows of fluids with Prandtl number less than unity are caused to become inviscidly unstable by a streamwise vortex restructuring of the flow.

### Acknowledgement

The author acknowledges support of SERC.



## References

- [1] Chen, K. and Cheng, M. M., 1984. Thermal instability of forced boundary layers. *Journal of Heat Transfer* **106**, pp. 284-289.
- [2] Denier, J., 1992. The Taylor vortex problem in the small wavelength limit. To appear in *IMA Journal of Applied Math.*
- [3] Hall, P., 1988. The nonlinear development of Görtler vortices in growing boundary layers. *J. Fluid Mech.* **193**, p. 243.
- [4] Hall, P. and Horseman, N.J. 1991 The linear secondary instability of longitudinal vortex structures in boundary layers. *J. Fluid Mech.* **232** p. 357.
- [5] Hall, P. and Morris, H., 1992. On the instability of boundary layers on heat flat plates. *J. Fluid Mech.* , accepted for publication.
- [6] Hall, P. and Lakin, W. D., 1988. The fully nonlinear development of Görtler vortices in growing boundary layers. *Proc. Roy. Soc. (A)* **415**, p. 441.
- [7] Hall, P. and Smith, F. T., 1991. On strongly nonlinear vortex/wave interaction in boundary layer transition. *J. FLuid Mech.* **227**, p. 641.
- [8] Moutsoglou, A., Chen, T. S. and Cheng, K. C., 1981. Vortex instability of mixed convection flow over a horizontal flat plate. *Journal of Heat Transfer* **103**, pp. 257-261.
- [9] Wu, R. S. and Cheng, K. C., 1976. Thermal instability of Blasius flow along horizontal plates. *Int. J. Heat Mass Transfer* **105**, pp. 907-913.

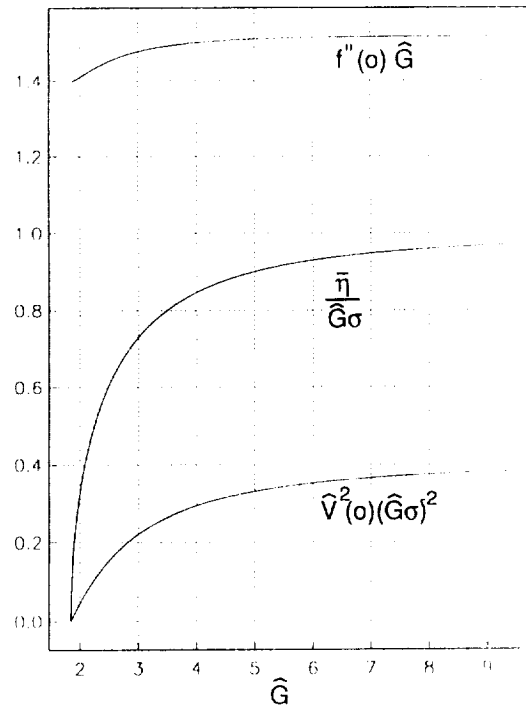


Figure 1a. The quantities  $f''(0)$ ,  $\hat{V}^2(0)$ ,  $\bar{\eta}$  for the similarity solution with  $\sigma = 1$ ,  $S = 0$ .

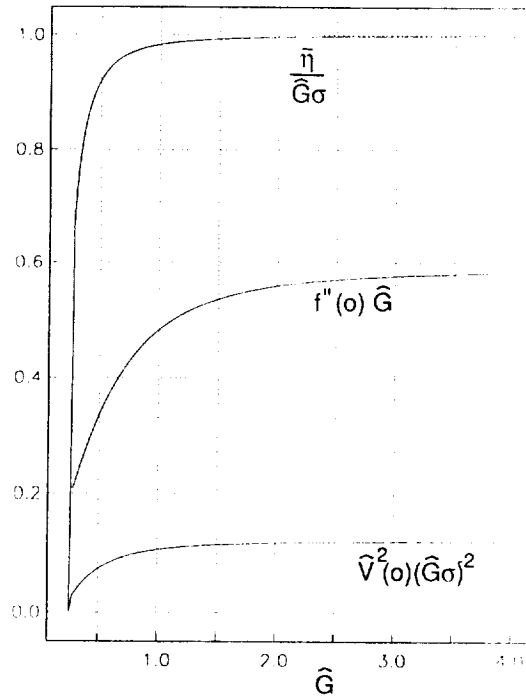


Figure 1b. The quantities  $f''(0)$ ,  $\hat{V}^2(0)$ ,  $\bar{\eta}$  for the similarity solution with  $\sigma = 5$ ,  $S = 0$ .

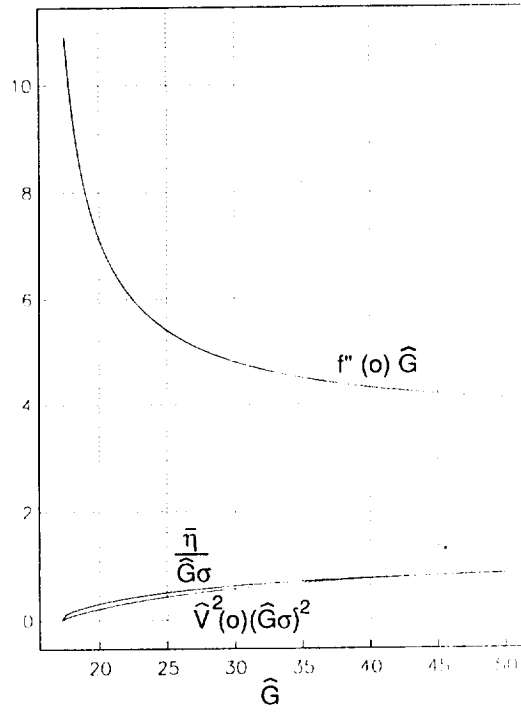


Figure 1c. The quantities  $f''(0)$ ,  $\hat{V}^2(0)$ ,  $\bar{\eta}$  for the similarity solution with  $\sigma = .2$ ,  $S = 0$ .

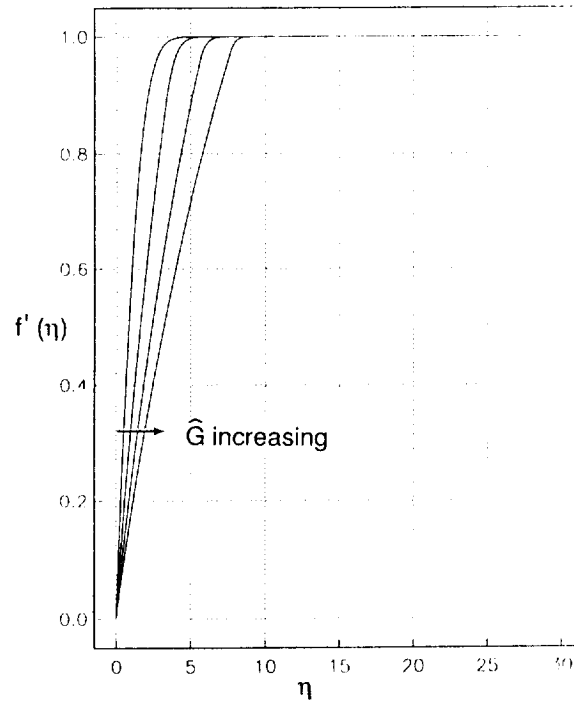


Figure 2a. The function  $f'(\eta)$  for  $S = 0$ ,  $\sigma = 1$ ,  $\hat{G} = 2, 4, 6, 8$ .

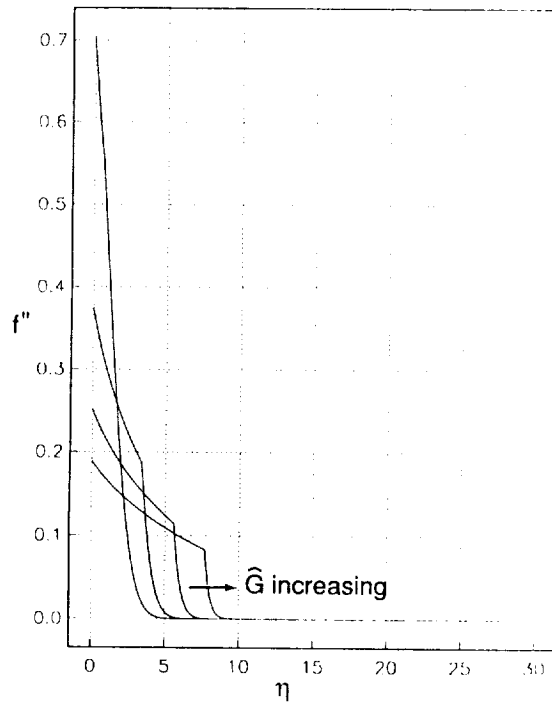


Figure 2b. The function  $f''(\eta)$  for  $S = 0$ ,  $\sigma = 1$ ,  $\hat{G} = 2, 4, 6, 8$ .

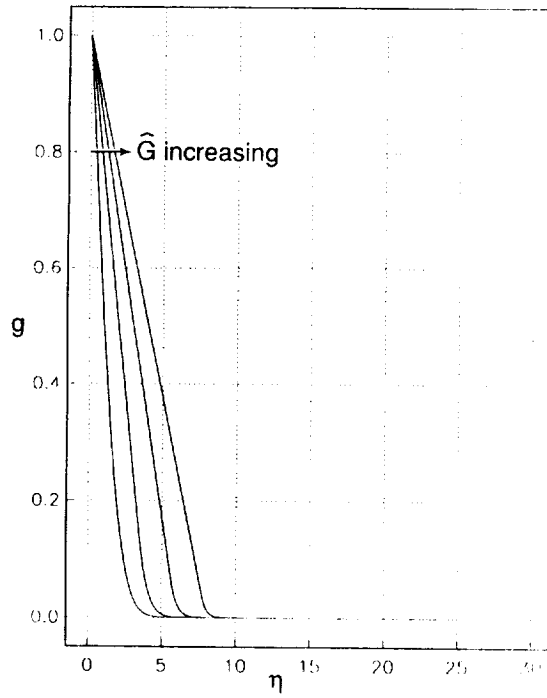


Figure 2c. The function  $g(\eta)$  for  $S = 0$ ,  $\sigma = 1$ ,  $\hat{G} = 2, 4, 6, 8$ .

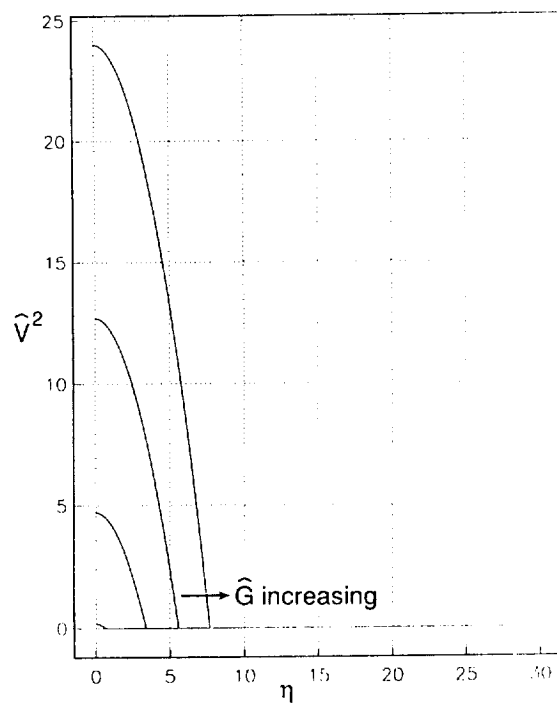


Figure 2d. The function  $\hat{V}^2(\eta)$  for  $S = 0$ ,  $\sigma = 1$ ,  $\hat{G} = 2, 4, 6, 8$ .

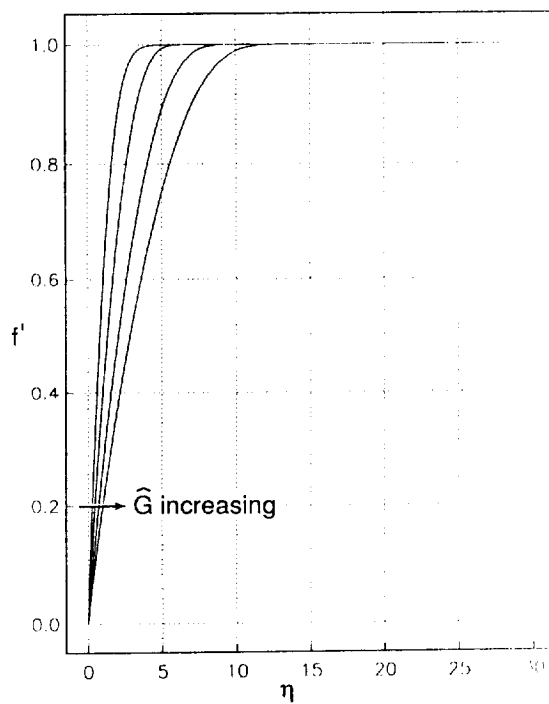


Figure 3a. The function  $f'(\eta)$  for  $S = 0$ ,  $\sigma = 5$ ,  $\hat{G} = .3, 1.1, 1.9, 2.7$ .

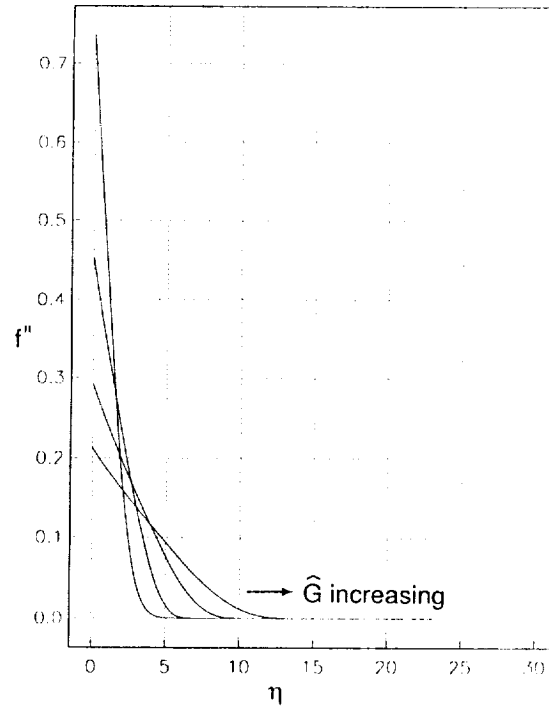


Figure 3b. The function  $f''(\eta)$  for  $S = 0$ ,  $\sigma = 5$ ,  $\hat{G} = .3, 1.1, 1.9, 2.7$ .

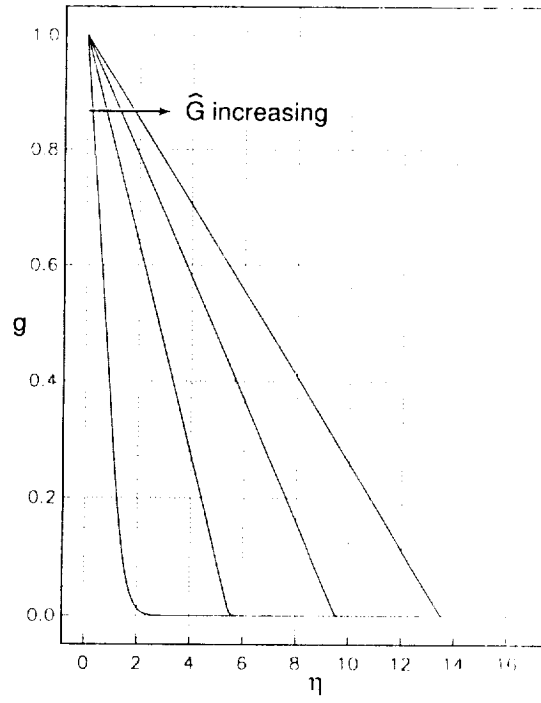


Figure 3c. The function  $g(\eta)$  for  $S = 0$ ,  $\sigma = 5$ ,  $\hat{G} = .3, 1.1, 1.9, 2.7$ .

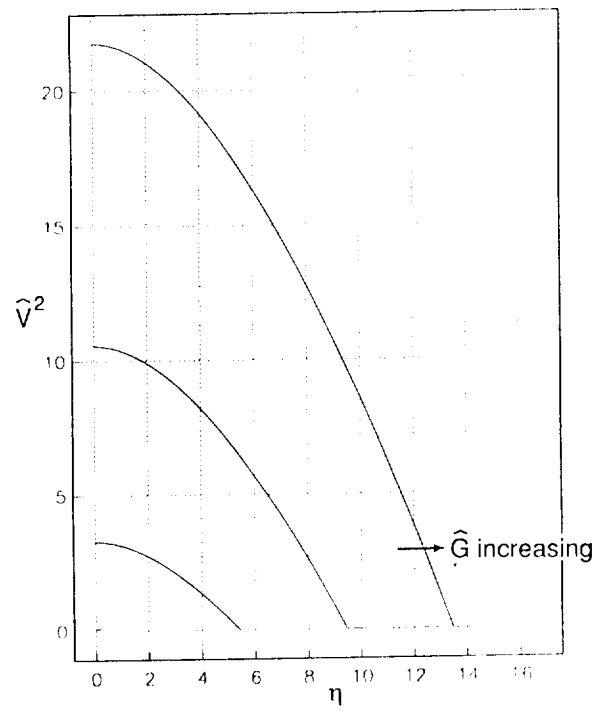


Figure 3d. The function  $\hat{V}^2(\eta)$  for  $S = 0$ ,  $\sigma = 5$ ,  $\hat{G} = .3, 1.1, 1.9, 2.7$ .

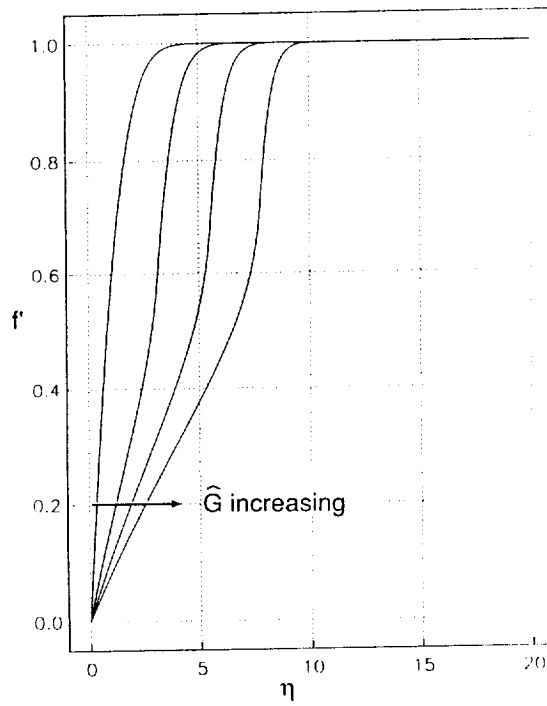


Figure 4a. The function  $f'(\eta)$  for  $S = 0$ ,  $\sigma = .2$ ,  $\hat{G} = 17.5, 27.5, 37.5, 47.5$ .

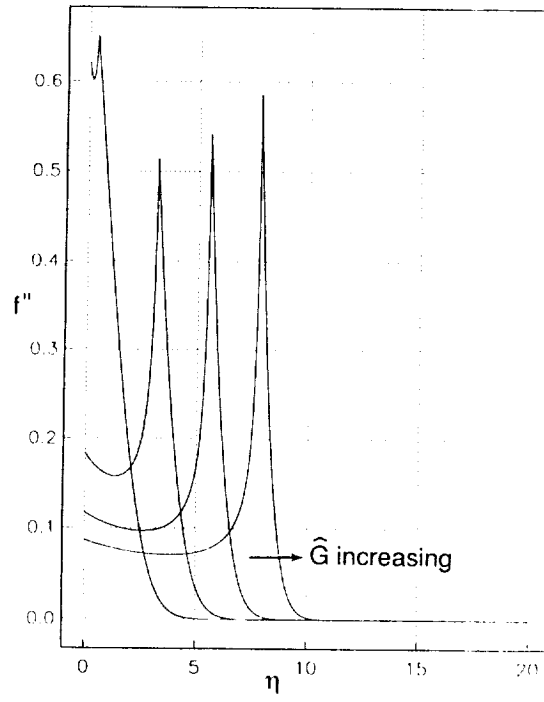


Figure 4b. The function  $f''(\eta)$  for  $S = 0$ ,  $\sigma = .2$ ,  $\hat{G} = 17.5, 27.5, 37.5, 47.5$ .

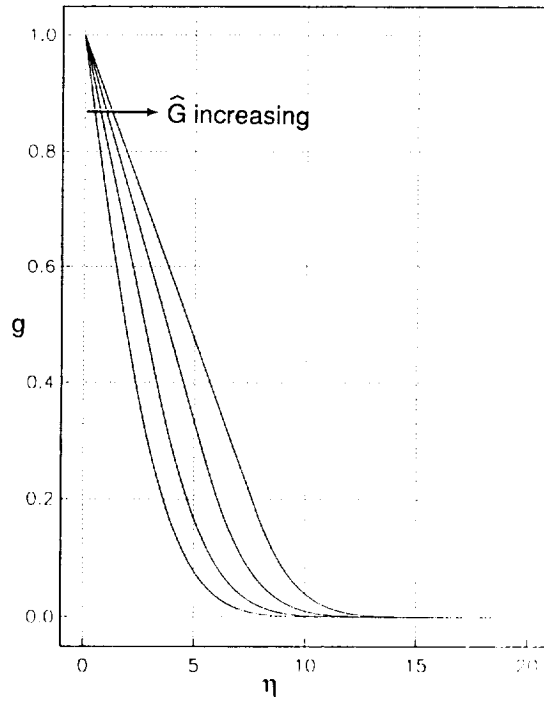


Figure 4c. The function  $g(\eta)$  for  $S = 0$ ,  $\sigma = .2$ ,  $\hat{G} = 17.5, 27.5, 37.5, 47.5$ .



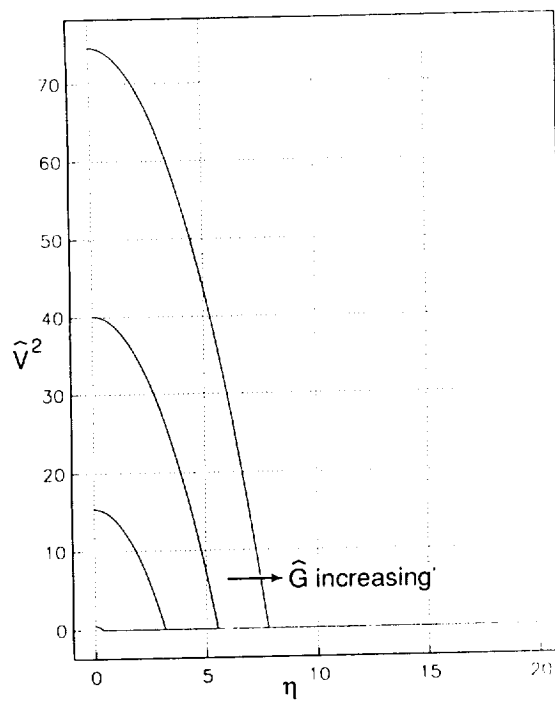


Figure 4d. The function  $\hat{V}^2(\eta)$  for  $S = 0$ ,  $\sigma = .2$ ,  $\hat{G} = 17.5, 27.5, 37.5, 47.5$ .

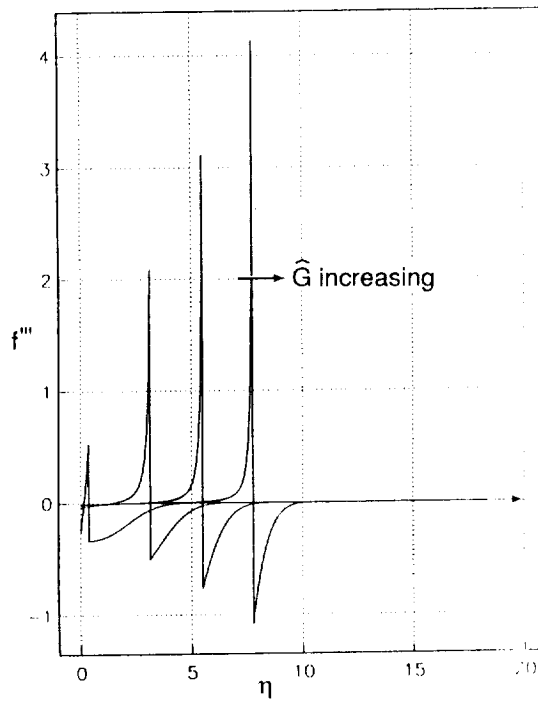


Figure 5. The function  $f'''(\eta)$  for  $S = 0$ ,  $\sigma = .2$ ,  $\hat{G} = 17.5, 27.5, 37.5, 47.5$ .

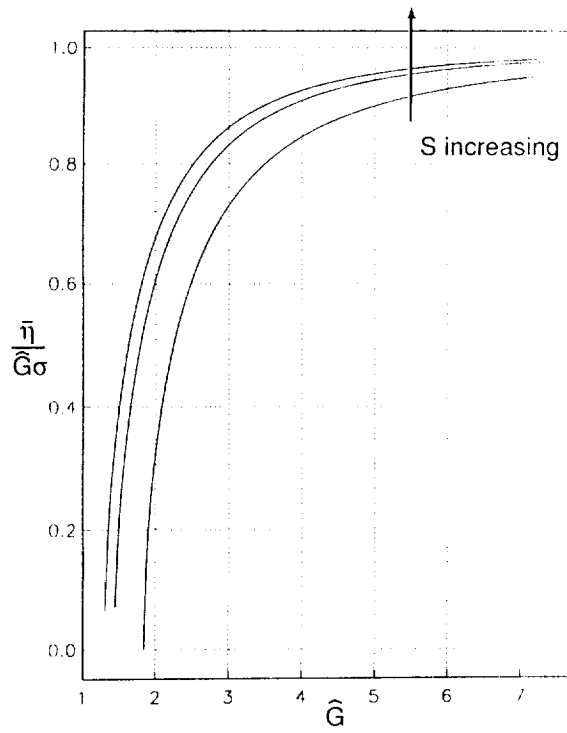


Figure 6a. The quantity  $\bar{\eta}$  for the similarity solution with  $S = 0, 1, 2$ ,  $\sigma = 1$ .

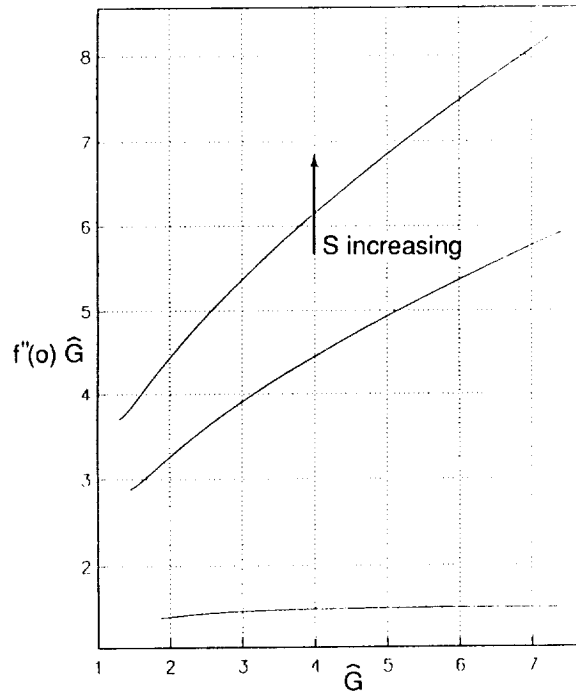


Figure 6b. The quantity  $f''(0)$  for the similarity solution with  $S = 0, 1, 2$ ,  $\sigma = 1$ .

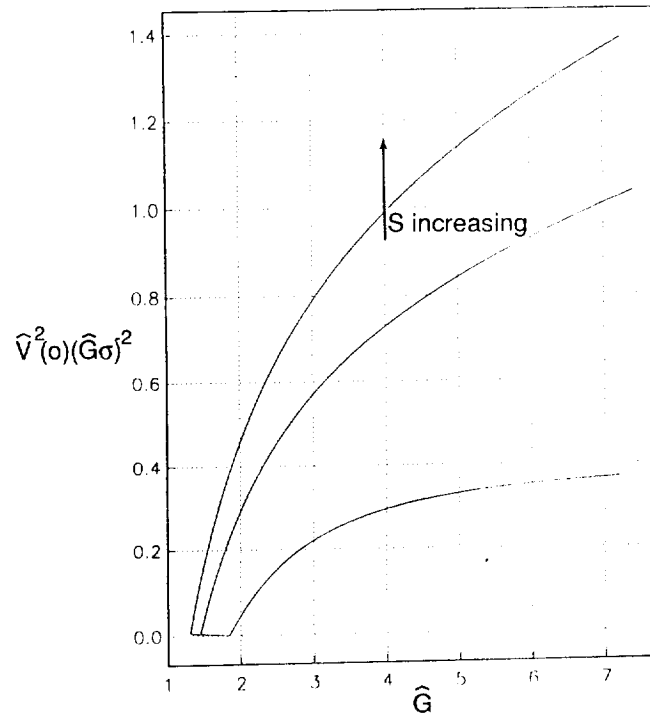


Figure 6c. The quantity  $\hat{V}^2(0)$  for the similarity solution with  $S = 0, .1, 2$ ,  $\sigma = 0$ .

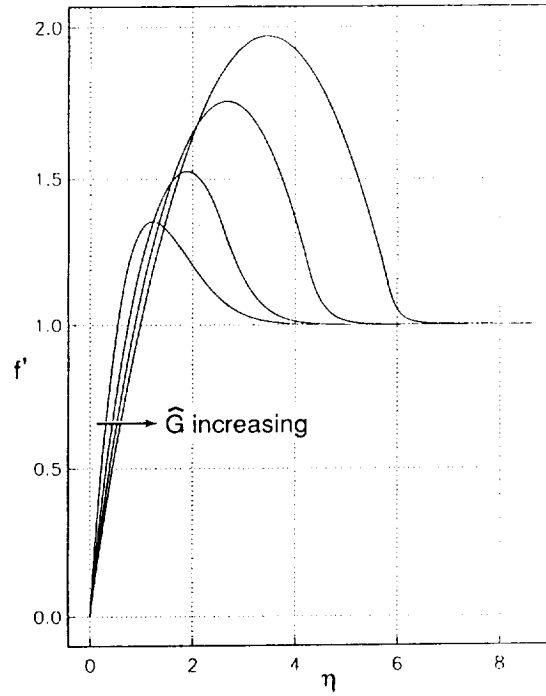


Figure 6d. The function  $f'(\eta)$  for  $\sigma = 1$ ,  $S = 2$  and  $\hat{G} = 1.5, 3, 4.5, 6$ .

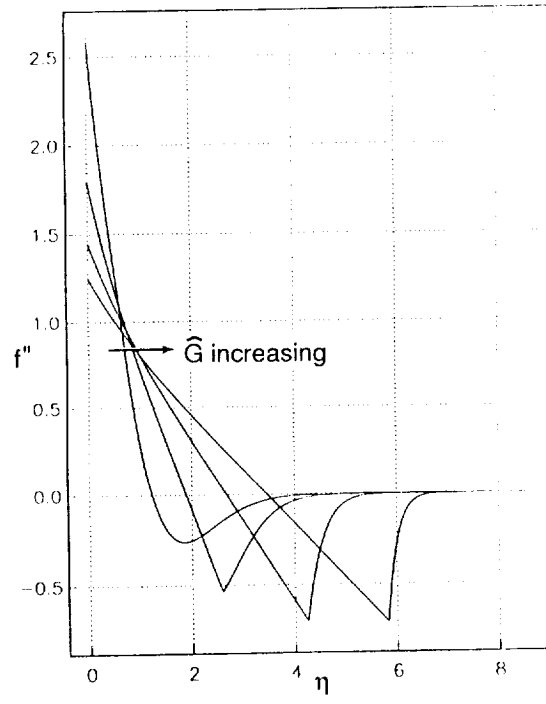


Figure 6e. The function  $f''(\eta)$  for  $\sigma = 1$ ,  $S = 2$  and  $\hat{G} = 1.5, 3, 4.5, 6$ .

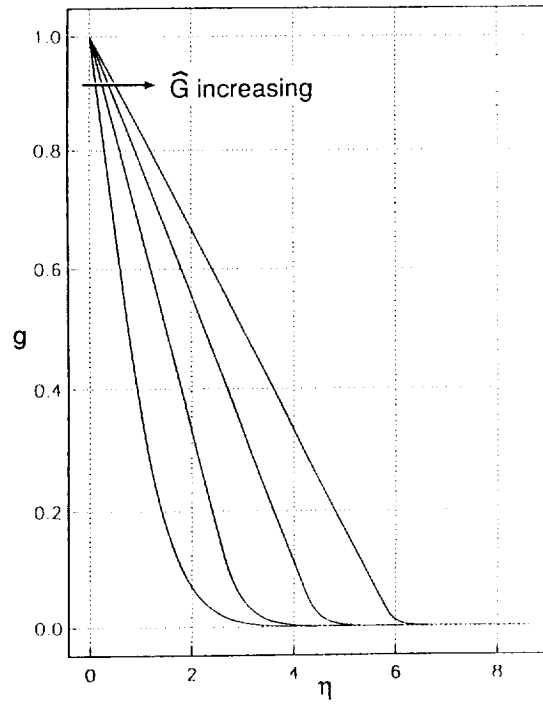


Figure 6f. The function  $g(\eta)$  for  $\sigma = 1$ ,  $S = 2$  and  $\hat{G} = 1.5, 3, 4.5, 6$ .

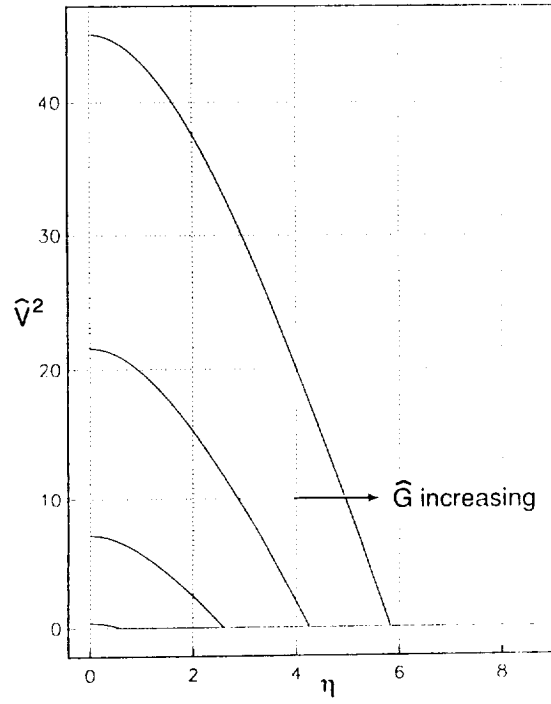


Figure 6g. The function  $\hat{V}^2(\eta)$  for  $\sigma = 1$ ,  $S = 2$  and  $\hat{G} = 1.5, 3, 4.5, 6$ .

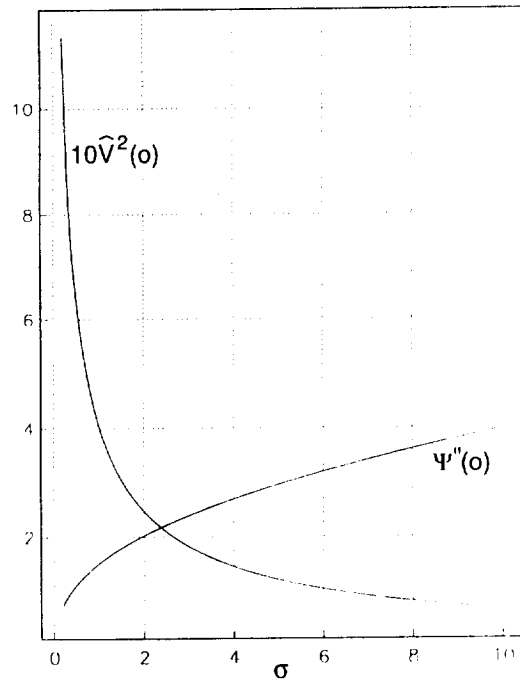


Figure 7. The quantities  $\Psi''(0)$ ,  $\hat{V}(0)$  as functions of  $\sigma$ .

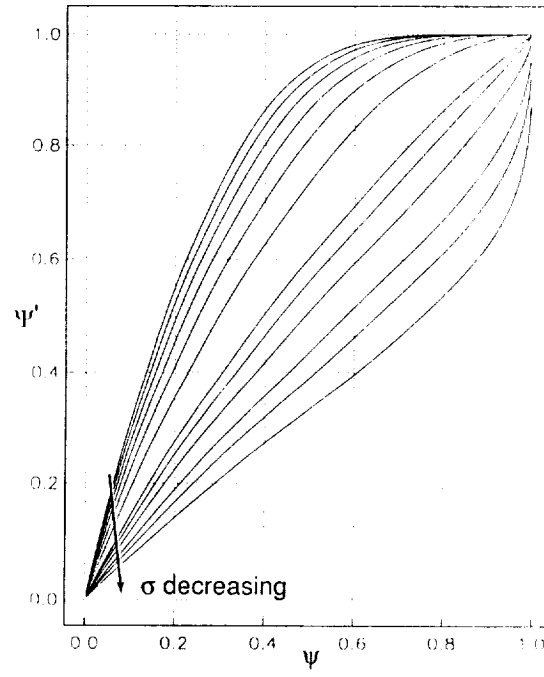


Figure 8a. The function  $\Psi'(\psi)$ , for  $S = 0$ ,  $\sigma = .2, .3, .4, .6, .8, 1, 2, 3, 4, 5, 6$ .

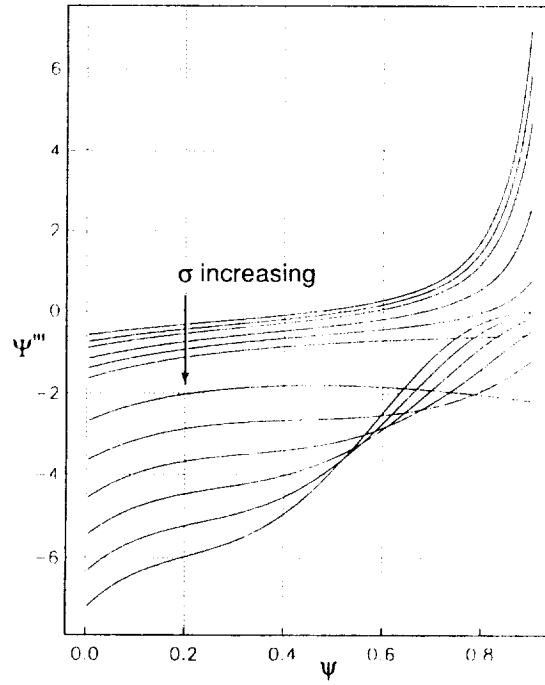


Figure 8b. The function  $\Psi'''(\psi)$ , for  $S = 0$ ,  $\sigma = .2, .3, .4, .6, .8, 1, 2, 3, 4, 5, 6$ .

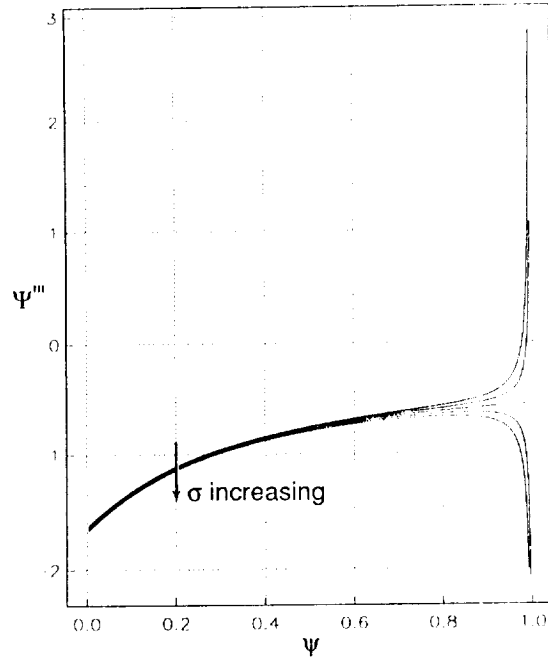


Figure 9. The function  $\Psi'''(\psi)$ , for  $S = 0$ ,  $\sigma = .98, .99, 1., 1.01, 1.02$ .

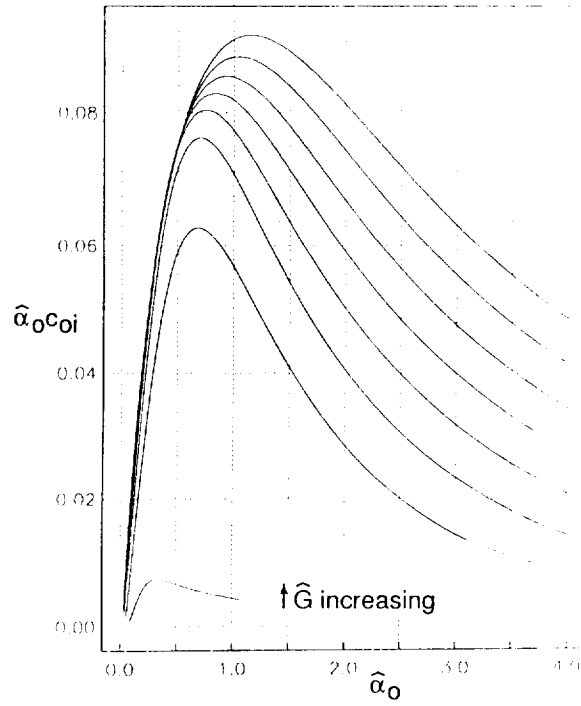


Figure 10. The growth rate  $\hat{\alpha}_0 \hat{c}_{0i}$  as a function of  $\hat{\alpha}_0$  for the case  $S = 0$ ,  $\sigma = .2$ , and  $\hat{G} = 17.5, 22.88, 24.88, 28.88, 32.88, 36.88, 40.88, 44.88$ .

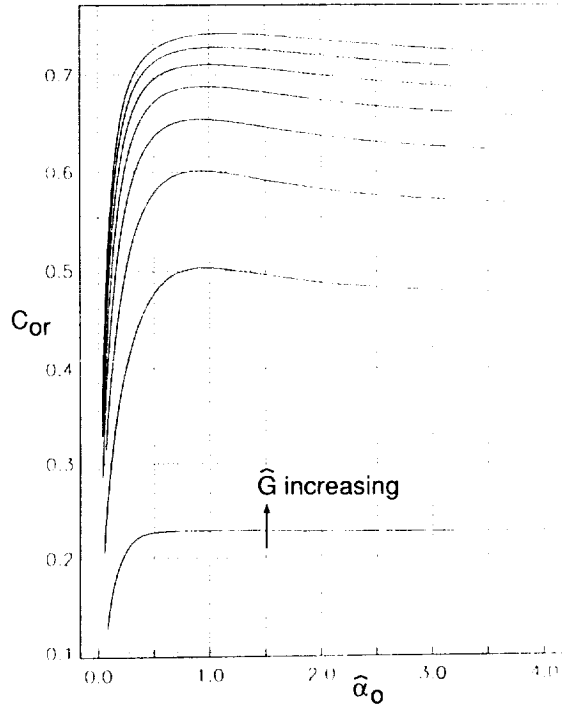


Figure 11. The wavespeed  $c_{0r}$  as a function of  $\hat{\alpha}_0$  for the case  $S = 0$ ,  $\sigma = .2$ , and  $\hat{G} = 17.5, 22.88, 24.88, 28.88, 32.88, 36.88, 40.88, 44.88$ .

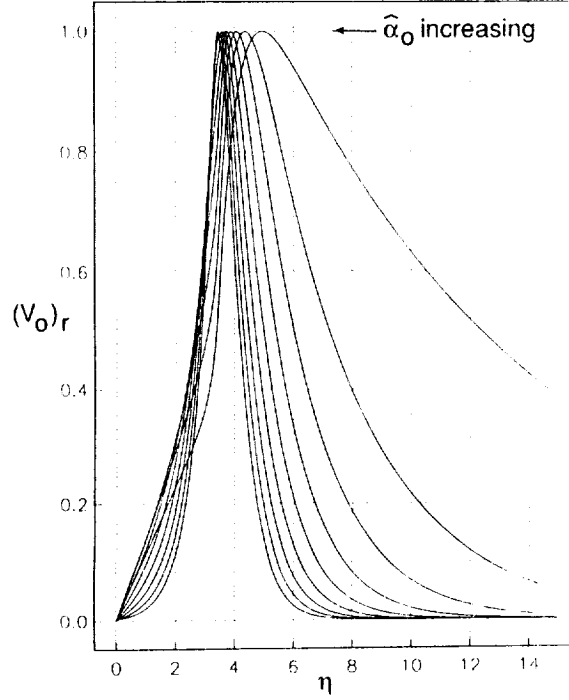


Figure 12. The real part of the eigenfunction  $V_0 = \frac{-P'_0}{i\hat{\alpha}_0(\bar{u}-\bar{c}_0)}$  as a function of  $\eta$  for  $S = 0$ ,  $\sigma = .2$ ,  $\hat{G} = 28.83$  and  $\hat{\alpha}_0 = .1, .3, .5, .7, .9, 1.1, 1.3, 1.5, 1.7, 1.9$ .



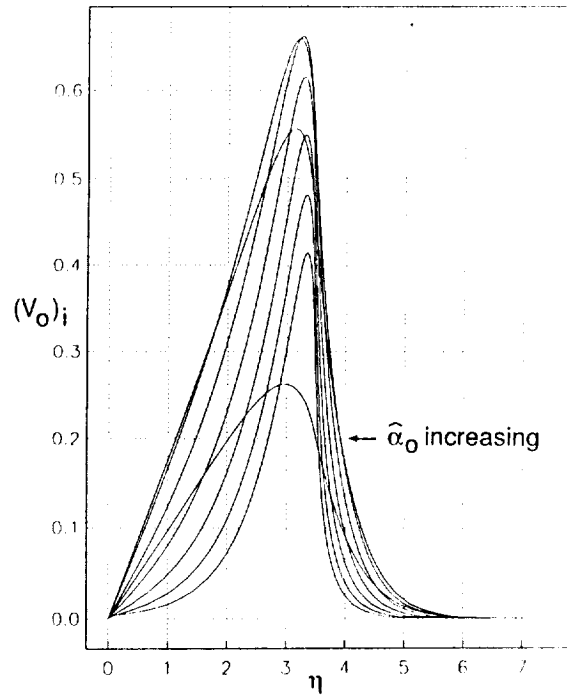


Figure 13. The imaginary part of the eigenfunction  $V_0 = \frac{-P'_0}{i\hat{\alpha}_0(\bar{u}-\hat{c}_0)}$  as a function of  $\eta$  for  $S = 0$ ,  $\sigma = .2$ ,  $\hat{G} = 28.83$  and  $\hat{\alpha}_0 = .1, .3, .5, .7, .9, 1.1, 1.3, 1.5, 1.7, 1.9$ .

REPORT DOCUMENTATION PAGE			Form Approved OMB No. 0704-0188	
Public reporting burden for this collection of information is estimated to average 1 hour per response, including the time for reviewing instructions, searching existing data sources, gathering and maintaining the data needed, and completing and reviewing the collection of information. Send comments regarding this burden estimate or any other aspect of this collection of information, including suggestions for reducing this burden, to Washington Headquarters Services, Directorate for Information Operations and Reports, 1215 Jefferson Davis Highway, Suite 1204, Arlington, VA 22202-4302, and to the Office of Management and Budget, Paperwork Reduction Project (0704-0188), Washington, DC 20503.				
1. AGENCY USE ONLY (Leave blank)	2. REPORT DATE June 1992	3. REPORT TYPE AND DATES COVERED Contractor Report		
4. TITLE AND SUBTITLE STREAMWISE VORTICES IN HEATED BOUNDARY LAYERS		5. FUNDING NUMBERS C NAS1-18605  WU 505-90-52-01		
6. AUTHOR(S) Philip Hall				
7. PERFORMING ORGANIZATION NAME(S) AND ADDRESS(ES) Institute for Computer Applications in Science and Engineering Mail Stop 132C, NASA Langley Research Center Hampton, VA 23665-5225		8. PERFORMING ORGANIZATION REPORT NUMBER  ICASE Report No. 92-23		
9. SPONSORING/MONITORING AGENCY NAME(S) AND ADDRESS(ES) National Aeronautics and Space Administration Langley Research Center Hampton, VA 23665-5225		10. SPONSORING/MONITORING AGENCY REPORT NUMBER  NASA CR-189661 ICASE Report No. 92-23		
11. SUPPLEMENTARY NOTES Langley Technical Monitor: Michael F. Card Final Report Submitted to Journal of Fluid Mechanics				
12a. DISTRIBUTION / AVAILABILITY STATEMENT Unclassified - Unlimited  Subject Category 34		12b. DISTRIBUTION CODE		
13. ABSTRACT (Maximum 200 words) The nonlinear instability of the boundary layer on a heated plate placed in an on-coming flow is investigated. Such flows are unstable to stationary vortex instabilities and inviscid traveling wave disturbances governed by the Taylor-Goldstein equation. For small temperature differences the Taylor-Goldstein equation reduces to Rayleigh's equation. When the temperature difference between the wall and free stream is small the preferred mode of instability is a streamwise vortex. It is shown in this case that the vortex, assumed to be of small wavelength, restructures the underlying mean flow to produce a profile which can be massively unstable to inviscid traveling waves. The mean state is shown to be destabilized or stabilized to inviscid waves depending on whether the Prandtl number is less or greater than unity.				
14. SUBJECT TERMS  streamwise vortices; heated boundary layers; inviscid traveling waves		15. NUMBER OF PAGES 39		
		16. PRICE CODE A03		
17. SECURITY CLASSIFICATION OF REPORT Unclassified	18. SECURITY CLASSIFICATION OF THIS PAGE Unclassified	19. SECURITY CLASSIFICATION OF ABSTRACT	20. LIMITATION OF ABSTRACT	



